
Electronic Thesis and Dissertation Repository

7-17-2019 1:00 PM

Identifying *Brachypodium distachyon* proteins interacting with histone deacetylase BdHD1

Alberto Giovanni Torrez
The University of Western Ontario

Supervisor
Tian, Lining
The University of Western Ontario Co-Supervisor
Henry, Hugh A. L.
The University of Western Ontario

Graduate Program in Biology
A thesis submitted in partial fulfillment of the requirements for the degree in Master of Science
© Alberto Giovanni Torrez 2019

Follow this and additional works at: <https://ir.lib.uwo.ca/etd>



Part of the [Molecular Genetics Commons](#), and the [Plant Biology Commons](#)

Recommended Citation

Torrez, Alberto Giovanni, "Identifying *Brachypodium distachyon* proteins interacting with histone deacetylase BdHD1" (2019). *Electronic Thesis and Dissertation Repository*. 6344.
<https://ir.lib.uwo.ca/etd/6344>

This Dissertation/Thesis is brought to you for free and open access by Scholarship@Western. It has been accepted for inclusion in Electronic Thesis and Dissertation Repository by an authorized administrator of Scholarship@Western. For more information, please contact wlsadmin@uwo.ca.

Abstract

Current evidence has revealed the involvement of epigenetic mechanisms, including histone deacetylases (HDACs), in plant stress responses. In *Arabidopsis thaliana*, HDA19, belonging to the RPD3/HDA1 class, interacts with transcription factors to form repressor complexes. HDAC research mainly exists for dicotyledons, whereas research on monocotyledons is limited. *Brachypodium distachyon* is used as a model plant to investigate questions unique to monocot crops. BdHD1 is the closest homologous gene to HDA19 in *B. distachyon*. This study investigated potential protein-protein interactions between BdHD1 and each of BdMYB22, BdWRKY24, BdWRKY41, BdHOS15 and BdPP2C1. Interactions were investigated using yeast two-hybrid (Y2H) and bimolecular fluorescence complementation (BiFC). Y2H assays showed that BdHD1 strongly interacts with the WRKY transcription factor BdWRKY24, and this was confirmed via BiFC. Also, an interaction between BdHD1 and the SANT domain-containing protein BdMYB22 was identified via Y2H and confirmed via BiFC. No interaction was observed with BdHOS15. This research provides insights for the further discovery of BdHD1-complexes in *B. distachyon*.

Keywords

Histone deacetylase, BdHD1, protein-protein interactions, monocot, *Brachypodium*

Acknowledgments

I would like to thank my supervisor Dr. Lining Tian for allowing me the opportunity to conduct this research. During my time in your lab, I have gained valuable experiences to aid in my growth as a researcher. I have improved my critical thinking, technical and communication skills during the completion of this project. I would like to thank my co-supervisor Dr. Hugh Henry, and my advisory committee members Dr. Abdelali Hannoufa and Dr. Danielle Way, for their valuable input throughout my research.

I would like to extend a special thanks to all the members of Dr. Tian's lab as you provided generous sources of scientific knowledge from which to consult. I appreciate the various experimental techniques and skills which you have shown me. I would not have been able to complete my research without your expertise. I would like to especially thank Dr. Jingpu Song for your shared knowledge and mentorship during my research. You were always available to help me with any experimental issues.

I would like to thank my friends and colleagues I have made during this research. Whether it was helping troubleshoot any research issues or wanting to grab a few beers after a long week at the lab, I appreciate the gesture.

Lastly, I would like to thank my family for their continued support and encouragement during my research. You were always there when I needed to have someone to talk to or provide any help that I needed throughout especially when I broke my leg. I cherish everything you've done as this wouldn't have been possible without you.

Table of Contents

Abstract.....	i
Acknowledgments.....	ii
Table of Contents	iii
List of Tables	vi
List of Figures.....	vii
List of Appendices	viii
List of Abbreviations	ix
1 Introduction.....	1
1.1 Chromatin Structure.....	1
1.2 Epigenetic Regulatory Response to Abiotic Stress.....	1
1.3 Post-Translational Histone Modifications	2
1.4 Histone Acetylation and Deacetylation	3
1.4.1 Histone Acetyltransferases.....	4
1.4.2 Histone Deacetylases	5
1.5 Plant Histone Deacetylases.....	5
1.6 HDAC Protein-Protein Interactions	6
1.6.1 Interactions with MYB Transcription Factors	7
1.6.2 Interactions with WRKY Transcription Factors	8
1.6.3 Interactions with Protein Phosphatases.....	9
1.6.4 Interactions with HOS15.....	10
1.7 <i>Brachypodium distachyon</i> as a Monocot Model Plant	10
1.8 BdHD1: Positive Regulator of Drought Tolerance in <i>B. distachyon</i>	11
1.9 Research Objectives.....	12

2	Materials and Methods	13
2.1	Identification of candidate <i>Brachypodium distachyon</i> interacting proteins	13
2.2	<i>In silico</i> analysis of candidate proteins	13
2.3	<i>Brachypodium distachyon</i> growth conditions	14
2.4	RNA extraction and cDNA synthesis	14
2.5	Gateway® Primer Design	15
2.6	Preparation of Media for Bacterial Cultures	18
2.7	Gateway® Gene Cloning	18
2.8	Vector Construction	19
2.9	Confirmation of Vectors	21
2.10	Yeast Two Hybrid Assay	22
2.10.1	Preparation of Y2H Growth Media	22
2.10.2	Y2HGold Competent Cell Preparation	22
2.10.3	Transformation of Y2HGold Cells	23
2.10.4	Y2H Experimental Controls	23
2.11	Bimolecular Fluorescence Complementation Assay	24
3	Results	25
3.1	Identification of Homologous Proteins in <i>Brachypodium distachyon</i>	25
3.2	Structural Analysis of <i>B. distachyon</i> proteins	29
3.3	Gene Cloning of BdMYB22, BdWRKY24 and BdHOS15	32
3.4	Cloning of BdWRKY41 and BdPP2C1	34
3.5	Generation of <i>pGADT7</i> and <i>pGBKT7</i> Constructs	34
3.6	Yeast Two Hybrid (Y2H) Identifies BdHD1 Protein-Protein Interactions	37
3.7	Construction of <i>pEarleygate201-YN</i> and <i>pEarleygate202-YC</i> Constructs	41
3.8	BiFC confirms interactions between BdHD1 and the transcription factors BdMYB22 and BdWRKY24	44

4	Discussion	50
4.1	BdHD1 forms protein-protein interactions	50
4.2	Interactions between HDACs and MYB-like transcription factors in <i>Brachypodium distachyon</i>	52
4.3	Interactions between HDACs and WRKY transcription factors in <i>B. distachyon</i>	54
4.4	No interaction between BdHD1 and BdHOS15 observed	55
5	Future Perspectives	58
	References	60
	Curriculum Vitae	78

List of Tables

Table 2.1 Primers used in the Gateway gene cloning experiments	17
Table 2. Primers used in single colony PCR experiments	21

List of Figures

Figure 1.1. Post-translational acetylation targets on H3 and H4 histone tails.	3
Figure 2.1. Schematic diagram of Gateway® gene cloning.	20
Figure 3.1. Protein sequence alignment of <i>B. distachyon</i> proteins to <i>Arabidopsis</i> homologs.....	28
Figure 3.2. Key domains identified in candidate <i>B. distachyon</i> proteins.	30
Figure 3.3. Tertiary structures of <i>Brachypodium distachyon</i> proteins.....	31
Figure 3.4. Single colony PCR for <i>pDONRTM221</i> constructs.	33
Figure 3.5. Analysis of amplified <i>pGADT7</i> destination vector fragments.	35
Figure 3.6. Confirmation of <i>pGBKT7</i> destination vectors.	36
Figure 3.7. BdHD1 in <i>B. distachyon</i> interacts with BdMYB22 and BdWRKY24.....	41
Figure 3.8. Confirmation of <i>pEarleygate201-YN</i> destination vectors.	42
Figure 3.9. Confirmation of <i>pEarleygate202-YC</i> destination vectors.	43
Figure 3.10. BiFC confirms interactions between BdHD1 with each BdMYB22 and BdWRKY24.....	46
Figure 3.11. BdHD1 interacts with BdMYB22 and BdWRKY24.....	48

List of Appendices

Appendix 1: BdMYB22 Sequence.....	73
Appendix 2: BdWRKY24 Sequence	74
Appendix 3: BdWRKY41 Sequence	75
Appendix 4: BdHOS15 Sequence.....	75
Appendix 5: BdPP2C1 Sequence.....	77

List of Abbreviations

ABA	Abscisic acid
<i>Arabidopsis</i>	<i>Arabidopsis thaliana</i>
<i>attB</i>	Gateway cloning attachment site
<i>B. distachyon</i>	<i>Brachypodium distachyon</i>
BiFC	Bimolecular fluorescence complementation
cDNA	Complementary DNA
ddH ₂ O	Double distilled water
DDO	Double dropout (SD/-Leu/-Trp) medium
Dicot	Dicotyledon
DNA	Deoxyribonucleic acid
HAT	Histone acetyltransferase
HDAC	Histone deacetylase
K	Lysine (amino acid)
LB	Luria-Bertani
Monocot	Monocotyledon
<i>N. benthamiana</i>	<i>Nicotiana benthamiana</i>
<i>NptII</i>	Neomycin phosphotransferase
PCR	Polymerase chain reaction

PTM	Post-translational modification
QDO	Quadruple dropout (SD/-Leu/-Trp/-His/-Ade) medium
QDO/X/A	Quadruple dropout (SD/-Leu/-Trp/-His/-Ade) supplemented with X- α -gal and Aureobasidin A
RNA	Ribonucleic acid
RPD3/HDA1	Reduced potassium deficiency ³ /histone deacetylase1
YFP	Yellow fluorescent protein
Y2H	Yeast Two Hybrid

1 Introduction

1.1 Chromatin Structure

The vast array of genetic information in the nucleus is efficiently packaged into conserved condensed structures in eukaryotic cells. These complex structures – chromatin – are composed of DNA and histone proteins (Kornberg, 1974). The chromatin complex is made up of subunits called nucleosomes (Olins and Olins, 1978). Each nucleosome contains 147 base-pairs of DNA tightly wrapped around the histone octet (Luger et al., 1997). The histone octet contains two copies of each histone protein: H2A, H2B, H3 and H4 (Olins and Olins, 1978). The octet is composed of a tetramer that consists of two copies of histones H3 and H4 bound to two dimers of H2A and H2B (Liu et al., 2014). Each histone protein is characterized by a core globular protein domain and an amino acid tail protruding from the core (Isenberg, 1979). The compact nucleosome forms a 10 nm fiber structure strongly resembling a “beads on a string” model (Kornberg, 1974). The nucleosome, a conserved DNA packaging unit, is responsible for the compaction of approximately 90% of the DNA within cells (Luger et al., 1997). Histone proteins are subject to several different post-translational modifications which impact the compaction of the chromatin structure, resulting in alterations of gene expression (Allfrey et al., 1964; Littau et al., 1965).

1.2 Epigenetic Regulatory Response to Abiotic Stress

Plants are often subjected to several different abiotic stresses in their environment due to a lack of consistent optimal growing conditions. Common abiotic stresses include cold-stress, drought-stress and heat-stress. Plants are unable to simply relocate away from their stressors and thus must acclimate to changes in their environment. The responses to these stressors may take place via changes in gene transcriptional regulatory networks. Specifically, gene expression may be regulated by chromatin structural changes induced by epigenetic regulation (Fuchs et al., 2006). Epigenetic changes may involve the manipulation of the chromatin structure to alter gene expression without alterations to the DNA sequence (Loidl, 2004). These alterations to the chromatin structure may take many forms, including histone variants, histone post-translational modifications, and DNA methylation (Berger, 2007). Epigenetic changes can provide a

mechanism of long-term stress response, because the reprogrammed chromatin structure retains stress memory via priming (Grunstein, 1997). Furthermore, epigenetic changes are generally defined as being either mitotically or meiotically heritable (Chinnusamy and Zhu, 2009).

1.3 Post-Translational Histone Modifications

The components of the nucleosome, including DNA and histones, are both subject to epigenetic regulation. Post-translational modifications (PTMs) of histone N-terminal tails are among the most common epigenetic changes (Goll and Bestor, 2002). PTMs include the acetylation, methylation, phosphorylation, ubiquitination and biotinylation of several target amino acids on the protruding histone tail (Allfrey et al., 1964). These changes may either have positive or negative effects on gene expression levels. Whether gene expression is up-regulated or down-regulated by PTMs depends on the specific change which has occurred; specifically, whether the structure or charge of the histone tail is changed by the modification (Anderson et al., 2001). Generally, acetylation and ubiquitination tend to enhance transcriptional activity (Allfrey et al., 1964; Sridhar et al., 2007), whereas modifications such as biotinylation repress transcription (Camporeale et al., 2007). Histone tail modifications may alter the chromatin packing and thus influence the accessibility of the transcriptional machinery to the DNA promoter regions (Berger, 2007).

PTMs do not occur randomly as certain residues are more prone to modifications than others. Each amino acid of the histone tail can only facilitate a single PTM, because presence of a PTM will inhibit another modification from occurring on the same amino acid (Yang and Seto, 2007). However, histone modification cross-talk is often observed, because PTMs can facilitate further modifications on nearby amino acids to form an epigenetic state (Wang et al., 2008). For example, the methylation of H3K9 leads to the phosphorylation of H3S10, which promotes the acetylation of H3K14 (Rea et al., 2000). Together, PTMs combine to form the “histone code, acting to encode different epigenetic states influencing gene transcriptional activity (Turner, 2000).

1.4 Histone Acetylation and Deacetylation

The protruding histone tail is subject to chromatin structure altering PTMs, including histone acetylation (Allfrey et al., 1964). Histone acetylation refers to the reversible transfer of acetyl groups to the ϵ -amino group of lysine (K) residues (Yang and Seto, 2007). The typical acetylation targets are located on H3 and H4 histone tails; specifically, H3: K4, K9, K14, K18, and K23 and H4: K5, K8, K12, K16 and K20 (Figure 1.1) (Loidl, 2004).

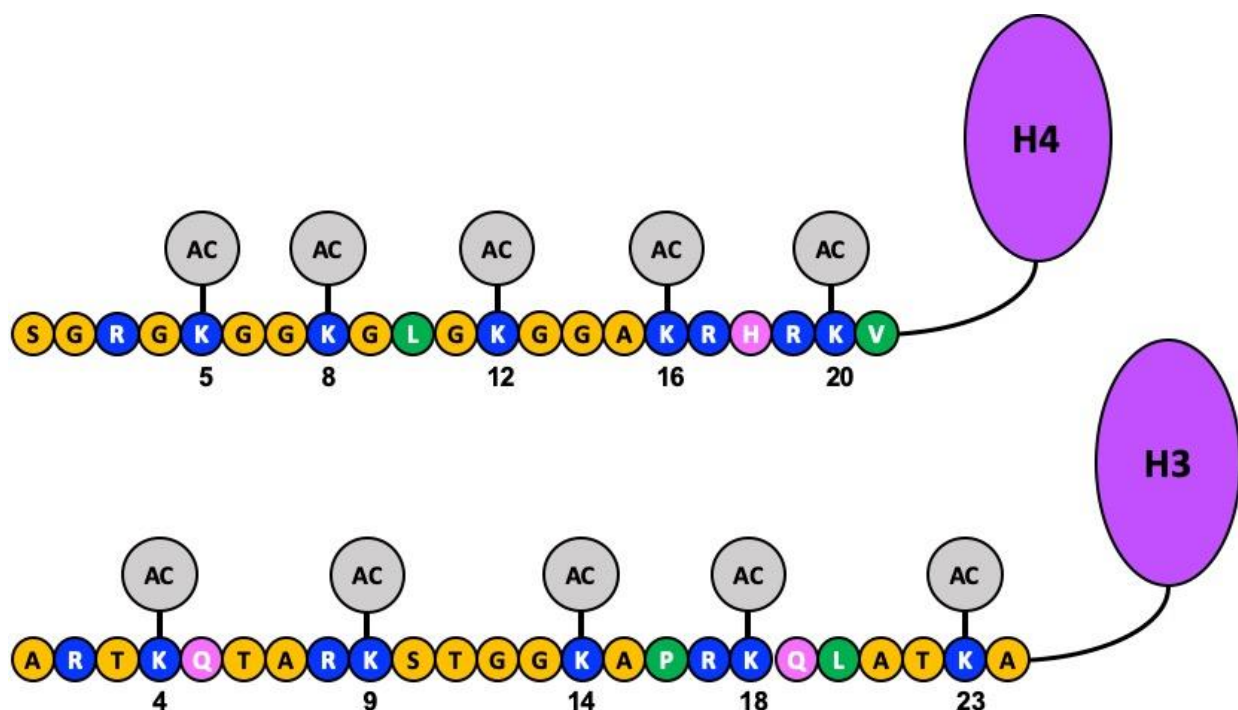


Figure 1.1. Post-translational acetylation targets on H3 and H4 histone tails.

Lysine residues on the histone H3 and H4 N-terminal tails are subject to reversible post-translational modifications, including acetylation. The acetylation of positively charged K residues neutralizes the charge to reduce the affinity to the DNA backbone. The Introduction to Bioinformatics (Lesk, 2014) amino acid colour scheme was used to represent small nonpolar (orange), hydrophobic (green), polar (magenta), negatively charged (red) and positively charged (blue) amino acid residues. Figure adapted from Loidl et al. (2004).

Histone acetylation physically alters the conformation of the chromatin structure. The positively charged K residues have a high affinity for the negatively charged DNA phosphate backbone in

the unacetylated state (Garcia-Ramirez et al., 1995). Acetylation decreases the affinity of the histone for DNA, because it neutralizes the charge of K (Garcia-Ramirez et al., 1995). In the hyperacetylated state the chromatin is open and transcriptionally active, because the promoter is accessible to the transcriptional machinery (Tian et al., 2005). Alternatively, deacetylation (the removal of the acetyl groups) increases the affinity of the K residues for the DNA backbone (Garcia-Ramirez et al., 1995). In the hypoacetylated state, the chromatin adopts a compact and transcriptionally repressed state (Tian et al., 2005). Generally, histone acetylation and deacetylation are associated with gene expression and repression, respectively. Histone acetylation is facilitated by a group of enzymes known as histone acetyltransferases (HATs), whereas histone deacetylation is conducted by histone deacetylases (HDACs) (Brownell and Allis, 1996). HATs and HDACs may act antagonistically to control the acetylation status of the histone tail, as observed with HISTONE ACETYLTRANSFERASE GCN5 (GCN5) and HISTONE DEACETYLASE 19 (HDA19) in *Arabidopsis thaliana* (Benhamed et al., 2006).

1.4.1 Histone Acetyltransferases

The transfer of acetyl groups from acetyl-CoA to the histone tail is facilitated by enzymes called histone acetyltransferases (HATs). HAT activity is associated with an open and transcriptionally active chromatin structure (Anderson et al., 2001). The hyperacetylated state of N-terminal lysine residues decreases the affinity of the positively charged histone tail for the negatively charged DNA phosphate backbone (Allfrey et al., 1964). Acetylation via HATs is not specific to histones; for example, tumor suppressor p53 and other general transcription factors are acetylated by HATs (Gu and Roeder, 1997; Yang and Seto, 2007).

HATs are classified into four different families: the GCN5-RELATED N-TERMINAL ACETYLTRANSFERASES (GNATs) family, the CREB-BINDING PROTEIN (p300/CBP) family, the MOZ, Ybf2/Sas3, Sas2 and Tip60 (MYST) family and the TATA-BINDING PROTEIN-ASSOCIATED FACTORS (TAF_{II}250) family (Pandey et al., 2002). The GNAT HATs contain a conserved HAT domain, as well as a bromodomain essential for targeted lysine binding (Haynes et al., 1992). Within HATs, the most conserved sequence, Q/RxxGxG, is important for binding and recognition of acetyl-CoA (Dutnall et al., 1998). Members of the MYST family are characterized by their zinc finger motifs, as well as the acetyl-CoA recognition sequence (Avvakumov and Cote, 2007). The CBP and TAF_{II}250 families contain fewer HATs.

Arabidopsis encodes twelve HATs; five each belong to the GNAT/MYST and CBP families, and two to the TAF_{II}250 family (Pandey et al., 2002). The activity of HATs is linked to several key processes, including development (Deng et al., 2007) and stress responses (Tan et al., 2019).

1.4.2 Histone Deacetylases

The acetylation of the histone tail is a reversible process facilitated by enzymes called histone deacetylases (HDACs). The typical targets of HDACs are histone lysine residues, thus lysine deacetylases (KDACs) may be used interchangeably to refer to HDACs (Choudhary et al., 2009). Histone deacetylation alters the histone-DNA interaction dynamics, resulting in a compact and transcriptionally repressed chromatin state (Garcia-Ramirez et al., 1995). The activity of HDACs coincides with gene repression (Kadosh and Struhl, 1998). HDACs act antagonistically to HATs by removing acetyl groups from residues of the N-terminal histone tails (Benhamed et al., 2006). Despite the name HDAC implying exclusive deacetylation from histones, other non-histone targets for deacetylation by HDACs have been identified, including tumor suppressor p53 (Gu and Roeder, 1997).

First discovered in yeast, HDACs are conserved proteins found in all eukaryotes (Vidal and Gaber, 1991). HDACs are classified into three distinct families, each classified on the basis of sequence similarity and co-factor dependency (Pandey et al., 2002). The three HDAC families are REDUCED POTASSIUM DEFICIENCY 3/ HISTONE DEACETYLASE 1 (RPD3/HDA1), SILENT INFORMATION REGULATOR 2 (SIR2) and HISTONE DEACETYLASE 2 (HD2) (Pandey et al., 2002). Members of the RPD3/HDA1 and SIR2 families are Zn²⁺ and NAD⁺ co-factor dependent, respectively (Imai et al., 2000; Wu et al., 2000). The RPD3/HDA1 and SIR2 families are conserved across all eukaryotes; meanwhile the HD2 family is a novel HDAC family unique to plants (Wu et al., 2000). *Arabidopsis thaliana* contains eighteen different HDAC genes (Hollender and Liu, 2008). Of the eighteen genes present, twelve belong to the RPD3/HDA1 family, and there are two SIR2 and four HD2 HDACs (Pandey et al., 2002; Hollender and Liu, 2008).

1.5 Plant Histone Deacetylases

Histone deacetylases are found within all eukaryotes, including plants, where they provide gene regulation in a variety of different processes. Diverse roles have been identified for plant HDACs

in several biological processes such as plant growth (Wu et al., 2008), biotic stress-responses including pathogen defense (Kim et al., 2008), and abiotic stress-responses such as salt-stress (Chen et al., 2010), heat-stress (Buszewicz et al., 2016) and drought-stress (Zheng et al., 2016). The subcellular localization of HDACs is typically nuclear, however cytoplasmic expression has been reported (Alinsug et al., 2012).

The most widely studied HDAC family is the RPD3 family, which is homologous to the yeast RPD3 (Kadosh and Struhl, 1998). Members of this family are characterized by the presence of the highly conserved histone deacetylase domain (Pandey et al., 2002). In both dicots and monocots the RPD3 family is the largest, with 12 and 14 members in *Arabidopsis* and *Oryza sativa* (rice), respectively (Hollender and Liu, 2008; Hu et al., 2009). The RPD3 family is subdivided into three classes based on sequence similarity: class I, class II and class III (Pandey et al., 2002).

The SIR2 and HD2 families are less common than the RPD3 family. The SIR2 family has a distinct structure to other HDACs, because it requires the co-factor NAD⁺. There are two members of the SIR2 family each in *Arabidopsis* and rice (Pandey et al., 2002; Hu et al., 2009). The last HDAC family, HD2, was first discovered in *Zea mays* (maize) (Lusser et al., 1997). This plant-specific HDAC family is represented by four and two members in *Arabidopsis* and rice (Pandey et al., 2002; Hu et al., 2009). HD2 HDACs are identified by a conserved amino acid terminal EFWG region required for repression activity (Wu et al., 2003).

1.6 HDAC Protein-Protein Interactions

Because many HDACs do not act individually, it is possible they function within protein to regulate gene expression. The common interacting partners for HDACs typically include proteins associated with the transcriptional machinery. For example, in yeast cells the transcriptional regulatory protein Ume6 – a DNA binding protein – recruits a complex containing SIN3, a co-repressor, and HDAC RPD3 to repress gene expression (Kadosh and Struhl, 1997). In *Arabidopsis*, LEUNIG (LUG) is a transcriptional co-repressor able to interact with an adaptor protein SUESS and HDA19 to repress transcription (Gonzalez et al., 2007). Protein interactions are important for functional activity; for example, LUG activity was significantly reduced following HDAC inhibition via trichostatin A (TSA) (Gonzalez et al., 2007). An interaction

between COI1 and HDA6 in *Arabidopsis* was reported; COI1 regulates the expression of jasmonate responsive genes via ubiquitination, targeting HDA6 for ubiquitination (Devoto et al., 2002).

Because HDAC activity is associated with transcriptional repression, the interacting partners of HDACs are generally transcriptional repressors. However, researchers have demonstrated the ability of HDACs to bind to activators and co-activators. The transcriptional activator SCARECROW (SCR) interacts with HDA19 under high auxin concentrations to reverse the repression by HDA19 on auxin responsive genes (Gao et al., 2004). HDA19 also can interact with the activator bnKCP1 in *Brassica napus* (Gao et al., 2003). Protein-protein interactions involving HDACs are required to target specific downstream genes for expressional changes.

1.6.1 Interactions with MYB Transcription Factors

Protein interactions are formed between HDACs and members of the MYB family and MYB-like transcription factors. The MYB family is a large conserved transcription factor family present across eukaryotes (Katiyar et al., 2012). The conserved MYB DNA-binding domain forms three α -helices arranged via a helix-turn-helix motif, which interacts with the major groove of the DNA backbone (Ogata et al., 1996). Members of the MYB family are grouped into four subfamilies based on the number of MYB repeats: 1R-, R2R3-, 3R- and 4R- (Dubos et al., 2010). The majority of MYB genes in rice and *Arabidopsis* belong to the plant specific MYB-R2R3 subfamily (Wilkins et al., 2008). The MYB family is a major transcription factor family with 155 and 197 members identified in rice and *Arabidopsis*, respectively (Katiyar et al., 2012). The general role of MYB genes include biologically important processes such as plant development (Dai et al., 2012), signal transduction (Abe et al., 1997), and responses to biotic (Cominelli et al., 2005) and abiotic stresses (Cominelli et al., 2005). MYB transcription factor functions overlap with HDAC gene regulation, however few interactions have been identified between them.

Limited research is available on interactions between HDACs and MYB proteins in plant systems. In mice, HDAC3 interacts in a protein complex involving the SMRT (silencing mediator of retinoid and thyroid hormone receptor) and NCoR (nuclear receptor corepressor) protein complexes to regulate gene expression in development and metabolism (Codina et al.,

2005). SMRT has a deacetylase activation domain (DAD), as well as a SANT-like domain (Codina et al., 2005). The SANT domain plays a role in chromatin remodeling as well as transcriptional regulation (Boyer et al., 2002). The SANT domain is similar in protein architecture to the MYB domain, however it cannot interact with DNA, because it does not possess the conserved basic residues on its surface required for DNA binding (Grüne et al., 2003). The identified DAD domain can bind directly to HDAC3, however the C-terminal SANT domain is required to mediate the interaction with the histone tails (Yu et al., 2003). In *Arabidopsis*, POWERDRESS (PWR) interacts with HDA9 (Chen et al., 2016). PWR contains the MYB-like SANT domain essential for HDA9 repression (Mayer et al., 2019). Interactions between MYB-like transcription factors such as the SANT domain-containing proteins with HDACs are highly likely, because the SANT domain is found in chromatin remodeling complexes.

1.6.2 Interactions with WRKY Transcription Factors

Among the largest transcription factor families is the plant-specific WRKY family (Rushton et al., 2010). The WRKY transcription factor family is characterized by the conserved WRKY domain, an amino acid sequence WRKYGQK found at the N-terminal end and the zinc-finger-like motif (Eulgem et al., 2000). The 60 amino acid conserved domain contains DNA-binding activity specific to the promoter W-box sequence, (T)TTGACC/T (Rushton et al., 1996). Members of the WRKY family have been studied within *Arabidopsis* and *Oryza sativa* (rice), identifying 72 and 105 members, respectively (Eulgem and Somssich, 2007; Zhang and Wang, 2005). Members are classified into either group I, II or III based on the number of WRKY domains and the structure of the zinc-finger-like motif (Eulgem et al., 2000). Proteins with two WRKY domains are classified as group I, whereas group II members have a single WRKY domain (Eulgem et al., 2000). The zinc-finger-like motif found in members of group I and II is C₂H₂, whereas group III members have a C₂-HC structure (Eulgem et al., 2000).

Interactions between plant HDACs and WRKYs have been identified previously. In *Arabidopsis*, WRKY38 and WRKY62 interact with HDA19 in response to pathogens (Kim et al., 2008). The WRKYs are transcriptional activators for downstream genes involved in suppression of the pathogen response; HDA19 interacts with WRKY38 and WRKY62 to abolish their activity, thus acting to positively regulate pathogen response (Kim et al., 2008). Furthermore a complex

between HDA9, WRKY53 and POWERDRESS (PWR) has been identified to regulate leaf senescence in *Arabidopsis* (Chen et al., 2016). A W-box motif was identified in HDA9 (Chen et al., 2016). HDA9 interacts with PWR, which is recruited by WRKY53 to W-box containing promoters. This suppresses negative regulation of leaf senescence, leading to the promotion of leaf senescence (Chen et al., 2016), although limited interactions between WRKYs and HDACs are clearly possible within *Arabidopsis*.

1.6.3 Interactions with Protein Phosphatases

The phosphorylation and dephosphorylation of HDACs are important in the regulation of HDAC activity. Serine/threonine protein phosphatases have been identified as interacting partners of several RPD3/HDA1 class HDACs via the dephosphorylation of serine and threonine residues (Wera and Hemmingst, 1995). In human HeLa cells, HDAC3 activity is down-regulated by an interaction with PROTEIN PHOSPHATASE 4 CATALYTIC SUBUNIT (PP4C) to dephosphorylate S424 (Zhang et al., 2005). An interaction between the catalytic domain of PROTEIN PHOSPHATASE 2 CATALYTIC SUBUNIT (PPP2CA) and HDAC2 in H9c2 cells was identified via immunoprecipitation (Yoon et al., 2018). The phosphorylation of S394 is required for HDAC2 activity (Eom et al., 2011); therefore, PPP2CA dephosphorylation plays an inhibitory role on HDAC2 activity (Yoon et al., 2018). In a similar fashion, PP2A can dephosphorylate HDAC7 to regulate its activity (Martin et al., 2008). The association of phosphatases and HDACs is observed in plants, as HDA14 interacts with PP2A in *Arabidopsis* (Martin et al., 2008). Generally, RPD3/HDA1 histone deacetylases interact with protein phosphatase to regulate HDAC activity.

In addition to the regulation of HDACs, protein phosphatases may interact with HDACs to co-repress downstream gene expression. For example, both HDA1 and PROTEIN PHOSPHATASE 1 (PP1) interact to dephosphorylate Ser133 of cAMP RESPONSIVE ELEMENT BINDING PROTEIN (CREB) in HEK293 cells (Canettieri et al., 2003). The HDAC-PP1 complex attenuates CREB activity via dephosphorylation of CREB, combined with the histone deacetylation of the promoter (Canettieri et al., 2003). This HDAC-PP1 complex illustrates the co-repression effects of both dephosphorylation and deacetylation working together in unison to regulate gene expression (Canettieri et al., 2003).

1.6.4 Interactions with HOS15

In *Arabidopsis*, interactions between HDACs with the protein HIGH EXPRESSION OF OSMOTICALLY RESPONSIVE GENE15 (HOS15) have been investigated. HOS15 is a negative regulator of stress-responsive genes (Zhu et al., 2008). HOS15 shares sequence similarity with the human histone interacting protein TRANSDUCIN-BETA LIKE (TBL); similar to TBL, HOS15 is able to interact with the H4 histone tail to mediate acetylation status (Zhu et al., 2008). In *hos15* transgenic lines, the acetylation status and expression of stress-related genes such as RD29A and ADH1 increases, implying reduced HDAC activity (Zhu et al., 2008). A complex involving an interaction between HOS15 and HDA9 to repress cold-response genes was identified; the complex binds to the promoter of GIGANTEA (GI) (Park et al., 2019). In *hda9-1* transgenic plants, the binding of HOS15 to the GI promoter was reduced, displaying the importance of the interaction with HDA9 (Park et al., 2019). Furthermore, a co-repression complex involving HOS15 and HD2C has been observed in *Arabidopsis* in response to cold stress (Park et al., 2018a). Interaction studies also have identified an interaction between HOS15 and HDA19 in *Arabidopsis* (Park et al., 2018b). Despite limited research, complexes involving HDAC and HOS15 interactions have been observed in plant systems.

1.7 *Brachypodium distachyon* as a Monocot Model Plant

Arabidopsis is traditionally used as a model organism for plant species. *Arabidopsis* is a dicotyledonous model system with many ideal characteristics for plant molecular research including a short life-cycle, physically small size and an annotated genome (Rhee et al., 2003). However, with an increasing number of sequenced genomes, more specific plant models are able to represent particular species of interest. For example, there is limited HDAC research in monocotyledon species, because most research has been conducted within dicotyledons such as *Arabidopsis*. Monocotyledons are of special interest, because they encompass several economically important cereal crops, including wheat, rice, corn, and barley. *Arabidopsis* is developmentally and physiologically different from cereal crops, requiring an alternative model for molecular research (Kellogg, 2015). *Arabidopsis* is distantly related to the family of grasses – Poaceae – which has not allowed for the successful identification of many genes of agronomic interest (Draper et al., 2001). The dependence of cereal crops for fuel and food production has presented the need for a closely related monocot model plant.

The members of Poaceae represent several agronomically important temperature cereals that tend to be physically large with long life-cycles, which is not ideal for molecular research purposes (Opanowicz et al., 2008). In order to perform molecular research and high-throughput genetic analysis an adequate model system was required (Draper et al., 2001). *O. sativa* has been used as a monocot model system for the Poaceae grass family, however its usage is questionable due to its long life-cycle and generally demanding growth conditions (Draper et al., 2001). Thus, *Brachypodium distachyon* has emerged a model species to study temperate cereals and related grasses.

B. distachyon is a monocot belonging to the grass subfamily Pooideae (Vogel et al., 2010). The subfamily Pooideae includes temperature cereals and forage grasses such as wheat, barley and oat, making *B. distachyon* an ideal model system relative to the more distantly related rice (Opanowicz et al., 2008). *B. distachyon* is an annual temperate grass native to the Middle East (Opanowicz et al., 2008). *B. distachyon* is among the simplest of grass genomes with a genomic size of 272 Mb, and five chromosomes are comparable to *Arabidopsis* (Opanowicz et al., 2008). With a short life-span of approximately three months, small stature (15-20 cm) and undemanding growth requirements, *B. distachyon* usage as a monocot model systems has increased over other plants such as rice and corn (Draper et al., 2001). Synteny between *B. distachyon* and other members of Poaceae has resulted in the identification of several conserved genomic regions, highlighting the effectiveness of this model system (Opanowicz et al., 2008). Combined, these factors have strengthened the status of *B. distachyon* as an effective model monocot system for investigating molecular biology research questions.

1.8 BdHD1: Positive Regulator of Drought Tolerance in *B. distachyon*

Through analysis of the *Brachypodium distachyon* genome, eight HATs and twelve HDACs were identified (Tan et al., 2019; Song et al., 2019). The twelve HDACs present in *B. distachyon* can be classified into two HDAC families, with eleven belonging to the RPD3/HDA1 family and one belonging to the HD2 family (Song et al., 2019). The histone deacetylase BdH1 (Bradi2g08060) is 78.2% similar at the protein level to HDA19 from *Arabidopsis* (Song et al., 2019). Both BdHD1 and HDA19 are classified as RPD3/HDA1 histone deacetylases based on sequence homology (Song et al., 2019). In *Arabidopsis*, HDA19, along with HDA6 and HDA9,

is responsive to drought (Chen and Wu, 2010). BdHD1 expression was sensitive to drought stress treatments in *B. distachyon* plants as expression levels increased (Song et al., 2019). In the BdHD1 overexpression lines OE22 and OE30, the survival of *B. distachyon* plants significantly increased under drought-stress conditions relative to wildtype Bd21-3 plants; decreased survival was observed in drought treatments for *bdhd1-30* plants (Song et al., 2019). BdHD1 plays a role in drought stress by positively regulating ABA sensitivity and drought tolerance (Song et al., 2019).

1.9 Research Objectives

HDACs do not function individually - they form protein complexes to properly regulate gene expression. In *B. distachyon*, BdHD1 shows high protein sequence similarity to HDA19 from *Arabidopsis* (Song et al., 2019). As previously demonstrated, HDA19 possesses the ability to form protein-protein interactions (Kim et al., 2008). For this study, I investigated protein-protein interactions between BdHD1 (Bradi2g08060) and candidate *B. distachyon* proteins, specifically BdMYB22 (Bradi2g01960), BdWRKY24 (Bradi2g49020), BdWRKY41 (Bradi2g53510), BdHOS15 (Bradi1g52640) and BdPP2C1 (Bradi2g45470). I hypothesized that BdHD1 would interact with the candidate *B. distachyon* proteins. The objective of this study was to identify candidate *B. distachyon* proteins that form protein-protein interactions with histone deacetylase BdHD1. The objective was accomplished by using *in silico* analysis to identify viable candidate interacting proteins. Once identified, interactions between BdHD1 and the candidate proteins were identified using the yeast two hybrid (Y2H) assay and confirmed via bimolecular fluorescence complementation (BiFC).

2 Materials and Methods

2.1 Identification of candidate *Brachypodium distachyon* interacting proteins

Brachypodium distachyon candidate interacting proteins were selected based on previous research and literary analysis. BdMYB22 (Bradi2g01960) and BdWRKY24 (Bradi2g49020) were selected based on unpublished research conducted in the Tian Lab at Agriculture and Agri-Food Canada's London Research and Development Centre by Jingpu Song; both proteins exhibited negative regulation in response to BdHD1 (Bradi3g08060) expression. BdWRKY41 (Bradi2g53510) was selected as a candidate interacting protein, because it belongs to the WRKY family of transcription factors, along with BdWRKY24. Previously, WRKY transcription factors have been reported to interact with HDACs in *Arabidopsis* (Kim et al., 2008). BdHOS15 (Bradi1g52640) a WD-40 protein, has recently been identified as a component of a gene regulating complex involving HDA9 (Park et al., 2019). Lastly, BdPP2C1 (Bradi2g45470) was selected as HDACs and serine/threonine protein phosphatases are known interacting partners that work together to repress gene expression (Wera and Hemmingst, 1995).

2.2 *In silico* analysis of candidate proteins

The key protein domains were identified within the candidate interacting *B. distachyon* proteins - BdMYB22, BdWRKY24, BdWRKY41, BdHOS15 and BdPP2C1 - using online resources. The amino acid sequence of each protein was obtained from *Phytozome.net* and input into *Protein BLAST®* (NCBI- National Center for Biotechnology Information, U.S. National Library of Medicine) to identify protein homologs present in *Arabidopsis thaliana*. The amino acid sequence alignment between each *Brachypodium* protein and its respective homolog was conducted using Clustal Omega (<https://www.ebi.ac.uk/Tools/msa/clustalo/>).

Further analysis and annotation of the key domains within each protein were conducted using the SMART (Simple Modular Architecture Research Tool) tool (<http://smart.embl-heidelberg.de/>). The functions of motifs present in each protein were provided by the SMART Tool. The Phyre2 tool (<http://www.sbg.bio.ic.ac.uk/phyre2>) was utilized to visualize the tertiary structures for each of the proteins investigated.

2.3 *Brachypodium distachyon* growth conditions

Wild-type *Brachypodium distachyon* Bd21-3 seeds were germinated for gene cloning purposes. The lemma was removed from the seeds, and the seeds were then soaked in ddH₂O for 2 hours at room temperature. The seeds were cold treated under dark conditions at 4 °C for 48 hours on damp filter paper to synchronize germination. After 2 days, germinated seedlings were subsequently transferred to a growth chamber with a 16-hour photoperiod, a light intensity of 75 μmol/m²/s, and a temperature of 25 °C, for 7 days.

Germinated seedlings were transferred to sterilized Magenta™ GA-7 Plant Tissue Culture Boxes (Sigma-Aldrich) containing 100 ml of modified Hoagland's hydroponic growth medium (49 mg/L H₃PO₄, 250 mg/L CaCl₂, 185 mg/L MgSO₄·7H₂O, 179 mg/L KCl, 58 mg/L NaCl, 241 mg/L NH₄Cl, 454 mg/L KNO₃, 2.86 g/L H₃BO₃, 1.81 g/L MnCl₂·4H₂O, 220 mg/L ZnSO₄·7H₂O, 51 mg/L CuSO₄, and 120 mg/L NaMoO₄·2H₂O in ddH₂O, pH=5.8). The seedlings were placed onto foam rafts with three plants per raft. Seedlings were placed through the raft holes ensuring the roots were fully submerged in the Hoagland's medium. Six *B. distachyon* plants were grown in each Magenta™ box. Plants were grown for three weeks in the Magenta™ boxes in a growth chamber with a 16-hour photoperiod with the parameters as previously stated. The hydroponic growth medium was changed every 7 days during the growth period.

2.4 RNA extraction and cDNA synthesis

The entirety of *B. distachyon* plant material was used for RNA extraction. Samples were collected after three weeks of growth in Hoagland's solution once they were approximately 7 cm in size. The samples were placed into 2 mL RNase-free microcentrifuge tubes with one Copperhead 6000 copper coated bead. The samples were frozen in liquid nitrogen and stored at -80 °C until RNA extraction was conducted.

RNA extraction was conducted using a Plant/Fungi Total RNA Purification Kit (Norgen Biotek Corp.), as per the product instructions. TissueLyser II (Qiagen) was used to homogenize the plant tissue to a fine powder. To lyse cells and inactivate RNases and proteases, 600 μL of Lysis Buffer C was added to the plant tissue and vortexed. After an incubation of 5 minutes at 55 °C, the lysate was spun through a Mini Filter Column to remove debris at 2 minutes at 14,000g. A

volume of 96-100% ethanol equal to the clear lysate was added, and subsequently loaded into the Spin Column provided by the kit. The spin column contains a resin with binding specificity for RNA, meanwhile DNA and proteins are removed in the flowthrough. The solution was centrifuged for 1 minute at 3,500g and the flowthrough was discarded. The RNA was washed using 400 μ L of Wash Solution A. Remaining impurities were removed from the RNA by centrifuging for 1 minute at 14,000g and the supernatant was discarded. Degradation of any DNA remaining in the samples was performed using 100 μ L of RNase-free DNase I (15 μ L DNase I and 100 μ L Enzyme Incubation Buffer) and centrifuged as mentioned in the previous step. An additional wash with Wash Solution A and a subsequent centrifugation was conducted. Finally, the purified total RNA was eluted by adding 30 μ L of Elution Solution A to the column. The column was placed into a fresh elution tube and the sample was spun for 2 minutes at 200g, followed by 2 minutes at 14,000g.

RNA concentration was measured using the NanodropTM 1000 Spectrophotometer. The concentration of the RNA samples ranged from 180-600 ng/ μ L. Complementary DNA (cDNA) synthesis from the extracted RNA was conducted using iScriptTM reverse transcription supermix (Bio-Rad, cat. 170-8841). The solution for reverse transcription was prepared (4 μ L iScriptTM reverse transcription supermix, 1000 ng total RNA, up to 20 μ L ddH₂O). The reverse transcription protocol was run on the EppendorfTM MastercyclerTM pro PCR system with the following parameters: 50 °C for 30 minutes to activate the reverse transcriptase, followed by 85 °C for 5 minutes to deactivate the enzyme. The cDNA was stored at -20 °C for short-term storage and -80 °C for long-term storage. The cDNA was used as the template for gene cloning in section 2.6.

2.5 Gateway® Primer Design

The primers for the *Brachypodium distachyon* genes were designed using online resources (*Phytozome.net*, *Primer3Plus*, *Primer-BLAST*). The identity of each gene was input into *Phytozome.net* in order to obtain the transcript sequence for each gene - BdHD1 (Bradi3g08060), BdMYB22 (Bradi2g01960), BdWRKY24 (Bradi2g49020), BdWRK41 (Bradi2g53510), BdHOS15 (Bradi1g52640) and BdPP2C1 (Bradi2g45470). The forward primers were designed to partially cover the 5' UTR and the transcription start site for the desired gene. The reverse

primers were located at the 3' end of the gene coding sequence with the omission of the termination sequence. Primers were designed using Primer3Plus (<http://www.bioinformatics.nl/cgi-bin/primer3plus/primer3plus.cgi>) and appropriately adjusting the parameters. The primer length was 18-20 base pairs, not inclusive of the Gateway® attachment sequences. In accordance with the Gateway® cloning manual the *attB1* sequence (5' ACAAGTTTGTACAAAAAAGCAG GCTNN 3') and the *attB2* sequence (5' ACCACTTTGTACAAAGCTGGGTN 3') were fused to the forward and reverse gene-specific primers, respectively (Hartley et al., 2000). The melting temperature and GC content were 60 °C and 40-60%, respectively. Suggested primer sequences obtained from *Primer3Plus* were input into *Primer-BLAST* (NCBI-National Center for Biotechnology Information, U.S. National Library of Medicine) to assess the specificity of the primers across the *B. distachyon* genome.

Table 2.1 Primers used in the Gateway gene cloning experiments

Primer Name	Primer Sequence (5' → 3')
BdHD1attF	GGGGACAAGTTTGTACAAAAAAGCAGGCTCAATGGACC TCTCCTCGGCC
BdHD1attR	GGGGACCACTTTGTACAAGAAAGCTGGGTATGGCTTCTG ATAAACAGCCGATG
BdMYB22attF	GGGGACAAGTTTGTACAAAAAAGCAGGCTCAATGCTAG TGCCATATCTGTCTATCT
BdMYB22attR	GGGGACCACTTTGTACAAGAAAGCTGGGTAGATTCCCTCC TGATCCCCACTC
BdWRKY24attF	GGGGACAAGTTTGTACAAAAAAGCAGGCTCAATGGATA ACCTCCACGGAGAGG
BdWRKY24attR	GGGGACCACTTTGTACAAGAAAGCTGGGTAGAACCGGG AGAGAAACTGAAGC
BdWRKY41attF	GGGGACAAGTTTGTACAAAAAAGCAGGCTCAATGCAGG CGCAGTCCC
BdWRKY41attR	GGGGACCACTTTGTACAAGAAAGCTGGGTAAAGCAGCA TGTCGTCGTCA
BdHOS15attF	GGGGACAAGTTTGTACAAAAAAGCAGGCTCAATGGGAG GGATTACATCGGC
BdHOS15attR	GGGGACCACTTTGTACAAGAAAGCTGGGTACATCCTGAA ATCCATGACACAGAC
BdPP2C1attF	GGGGACAAGTTTGTACAAAAAAGCAGGCTCAATGAGCA CCGAGACGACG
BdPP2C1attR	GGGGACCACTTTGTACAAGAAAGCTGGGTACCTGCGGTT CTCTTTGATCAC

2.6 Preparation of Media for Bacterial Cultures

Luria-Bertani (LB) medium was used to culture *Escherichia coli* (*E. coli*) and *Agrobacterium tumefaciens* (*A. tumefaciens*). Liquid LB medium was prepared using 5g/L BD Biosciences Bacto™ Yeast Extract (Ref. 212750), 10g/L BD Biosciences Bacto™ Tryptone (Ref. 211705), and 10g/L NaCl in ddH₂O. Solid LB medium was prepared as described above with the addition of 10g/L BD Biosciences Bacto™ Agar (Ref. 214010). LB plates used with pDONR221™, pEarleygate201-YN, pEarleygate202-YC, and pGBKT7 constructs were supplemented with 50µg/mL kanamycin (Sigma-Aldrich). Bacterial cultures containing pGADT7 were supplemented with 50µg/mL ampicillin (Sigma-Aldrich). LB medium used for *A. tumefaciens* was additionally supplemented with 50µg/mL rifamycin (Sigma-Aldrich).

2.7 Gateway® Gene Cloning

Gateway® cloning was used for gene cloning as per the product's instructions (Invitrogen). The BdMYB22 coding sequence was cloned using the BdMYB22attF and BdMYB22attR primers, (Table 2.1). The *attB* recombination sites fused to the primers acted as attachment sites for recombination of the cloned genes into the entry vector (Landy, 1989). BdMYB22 was cloned from the *B. distachyon* Bd21-3 cDNA template obtained in section 2.4. The PCR mix was prepared (13.3 µL ddH₂O, 5 µL 5X Green Buffer, 3 µL 25 mM MgCl₂, 0.5 µL DNTPs mix, 0.2 µL Taq DNA Polymerase, 1µL cDNA template and 1µL of each BdMYB22attF and BdMYB22attR primers). PCR experiments were carried out using the Eppendorf™ Mastercycler™ pro PCR system. The parameters for the PCR protocol included initialization at 94 °C for 2 minutes, followed by 30 cycles of denaturing at 94 °C for 15 seconds, annealing at 60 °C for 30 seconds and elongation for at 72 °C for 30 seconds, and a final elongation for 5 minutes at 72 °C. PCR products were loaded and visualized on 1% agarose gels. The gel was loaded with 10 µL of PCR product per lane and was run for 20 minutes at 140V using the ENDURO™ Gel XL Electrophoresis System.

The BdMYB22 coding sequence flanked by the *attB* recombination sites was transferred into the entry vector pDONR™221 using the Gateway® BP Clonase® (Thermo Fisher Scientific cat. 11789-020) reaction mix. The BP reaction was incubated overnight at 25 °C. Electroporation

was used to transfer the *pDONRTM221-BdMYB22* vector into electrocompetent *E. coli* strain DH5 α cells on LB medium. Transformed *E. coli* cells were incubated overnight at 37 °C. After incubation, the *pDONRTM221-BdMYB22* plasmids were then isolated and analyzed.

Single colony PCR was run using the M13-F vector specific forward primer and the gene specific BdMYB22 reverse primer. The parameters for the single colony PCR were as described above with the exception of an elongated initialization step at 94 °C for 10 mins. The *pDONRTM221-BdMYB22* was sequenced once the correct fragment size was identified via colony PCR. Sequencing analysis was done at AAFC (Agriculture and Agri-Food Canada, London Research and Development Centre). The *pDONRTM221-BdWRKY24* and *-BdHOS15* entry vectors were constructed using the methods mentioned above.

2.8 Vector Construction

The destination vectors used in the yeast two-hybrid (Y2H) and bimolecular fluorescence complementation (BiFC) were generated using Gateway® technologies (Earley et al., 2006) (Lu et al., 2010). For Y2H, the pGADT7-Gateway® and pGBKT7-Gateway® destination vectors were used, while pEarleygate201-YN and pEarleygate202-YC were used for BiFC. The BdMYB22 coding sequence was recombined into the destination vector pGADT7-Gateway® from the entry vector *pDONRTM221-BdMYB22* using the Gateway® LR Clonase® (Thermo Fisher Scientific cat. 11791-020) reaction mix. The LR reaction was incubated overnight at 4 °C. Electroporation was used to transfer the *pGADT7-BdMYB22* vector into *E. coli* strain DH5 α cells. *E. coli* cells were incubated overnight at 37 °C after transformation. The *pGADT7-BdMYB22* plasmids were isolated and confirmed via restriction enzyme digests and single colony PCR. Using the above methods *pDONRTM221-BdMYB22* was additionally recombined into each of pGBKT7-Gateway®, pEarleygate201-YN and pEarleygate202-YC. The destination vectors were generated as described above for BdHD1, BdWRKY24, and BdHOS15 sequences. For BdHD1 the *pDONRTM221-BdHD1* entry vector was constructed in the Tian Lab by Jingpu Song.

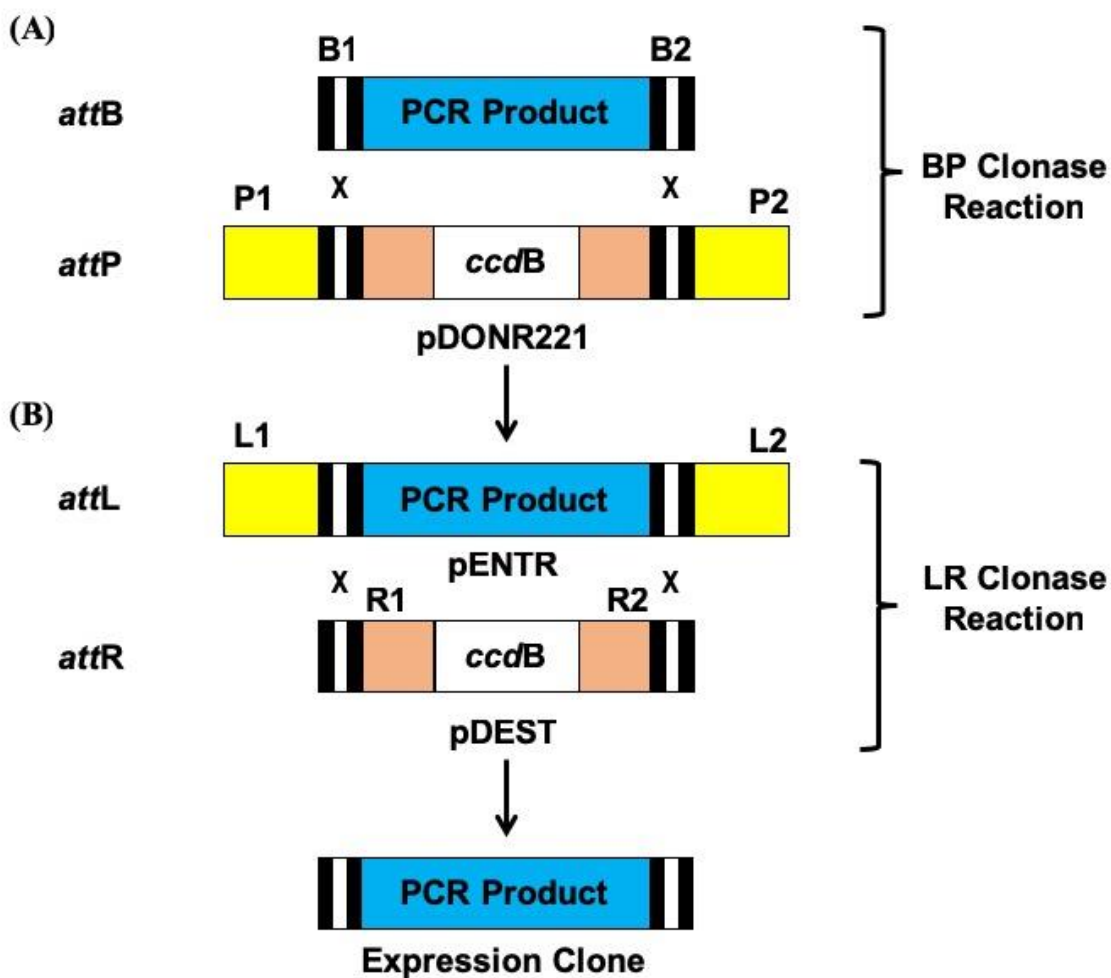


Figure 2.1. Schematic diagram of Gateway® gene cloning.

A, the gene coding sequence is flanked by the *attB1* and *attB2* Gateway® coding sequences. BP Clonase allows *attB* and *attP* sites to recombine, inserting the gene coding sequence into pDONR221 replacing the lethal *ccdB* gene. **B**, the entry vector, pENTR, contains the gene coding sequence flanked by the *attL1* and *attL2* sites. LR Clonase allows the *attL* sites to recombine with *attR* to insert the PCR product into the pDEST vector to produce the expression clone. Figure adapted from Karimi et al. (2007).

2.9 Confirmation of Vectors

To confirm the correct gene coding sequence was transferred into each destination vector, single colony PCR and RE digests were conducted. To isolate the pGADT7-BdMYB22 plasmids, single colonies of transformed *E. coli* strain DH5 α were selected. Single colony PCR was run using the T7-F vector specific forward primer and the gene specific BdMYB22 reverse primer. The parameters for the single colony PCR were as described in section 2.6. The T7-F primer was used for pGADT7 and pGBKT7 vector constructs, whereas the 35S-F primer was used for pEarleygate201-YN and pEarleygate202-YC constructs. The gene specific primers used for colony PCR did not contain the flanked *attB* sequence (Table 2).

Further confirmation was conducted using a double restriction digest using BamHI and EcoRV. The restriction digest mix was set up (2.5 μ L pGADT7-BdMYB22, 1 μ L 3.1 Buffer, 1 μ L BamHI, 1 μ L EcoRV, 5.5 μ L ddH₂O) and incubated at 37 °C for 2 hours. The incubation was followed by adding 2 μ L of Loading Dye. A volume of 10 μ L of each sample was run on a 1% agarose gel for 20 mins at 140 V. The same method was conducted for confirmation of all destination vectors – pGADT7, pGBKT7, pEarleygate201-YN, and pEarleygate202-YC, for each of BdHD1, BdMYB22, BdWRKY24, and BdHOS15.

Table 2. Primers used in single colony PCR experiments

Primer Name	Primer Sequence (5' \rightarrow 3')
M13-F	GTAAAACGACGGCCAGT
T7-F	TAATACGACTCACTATAGGGC
35S-F	CAATCCCACTATCCTTCGCAAGACCC
BdHD1-R	TGGCTTCTGATAAACAGCCGATG
BdMYB22-R	GATTCCTCCTGATCCCCACTC
BdWRKY24-R	GAACCGGGAGAGAACTGAAGC
BdHOS15-R	CATCCTGAAATCCATGACACAGAC

2.10 Yeast Two Hybrid Assay

2.10.1 Preparation of Y2H Growth Media

The Double Dropout medium: SD/-Leu/-Trp (DDO) plates for Y2H were prepared using 46.7 g/L Minimal synthetic defined (SD) Agar Base (Takara Bio #630411) and 0.64g/L -Leu/-Trp DO (Takara Bio #630417) supplement in ddH₂O. The medium was autoclaved prior, and then poured into plates. For Quadruple Dropout medium: SD/-Leu/-Trp/-His/-Ade (QDO) media, SD agar base was supplemented with 0.60 g/L -Ade/-His/-Leu/-Trp DO supplement (Takara Bio #630428) in ddH₂O. QDO medium supplemented with X- α -Gal and Aureobasidin A (QDO/X/A) was prepared similarly to QDO with the addition of 200 μ L Aureobasidin A stock solution and 1 ml X- α -Gal Stock solution (Takara Bio #630463) after autoclaving.

2.10.2 Y2HGold Competent Cell Preparation

Yeast two hybrid (Y2H) experiments were carried out according to the Yeastmaker™ Yeast Transformation System 2 User Manual (Takara Bio) to identify protein-protein interactions (Fields and Song, 1989) (Chien et al., 1991). The coding regions of BdHD1, BdMYB22, BdWRKY24 and BdHOS15 were cloned into both pGADT7-Gateway® and pGBKT7-Gateway®, according to section 2.7. The vectors for Y2H were transferred into *Saccharomyces cerevisiae* strain Y2HGold (Takara Bio). The competent yeast cells were prepared via overnight incubation at 30 °C in 3 mL of YPDA medium. After the incubation, 5 μ L of the yeast culture was added to 50 mL fresh YPDA and incubated until OD₆₀₀ reached 0.15-0.3. The cells were pelleted at 700g for 5 mins at room temperature and the supernatant was discarded. The culture was resuspended in 100 mL fresh YPDA and incubation was resumed until OD₆₀₀ reached 0.4-0.5. The cells were pelleted under the same parameters as the previous step and were resuspended in 30 mL sterile ddH₂O. The cells were pelleted a third time with the cells being resuspended in 1.5 mL of 1.1xTE/LiAc (1.1 mL 10x TE buffer, 1.1 mL 1M LiAc, 7.8 mL ddH₂O). This was followed by a final centrifugation with the competent cells resuspended in 600 μ L of 1.1xTE/LiAc.

2.10.3 Transformation of Y2HGold Cells

The transformation of the Y2H constructs was conducted once the competent cells were prepared. A concentration of 200 ng of each pGBKT7-DEST (bait) and pGADT7-DEST (prey) combination was added to 5 μ L of denatured YeastmakerTM Carrier DNA (Takara Bio). A mixture of *pGBKT7-BdHD1* with each of *pGADT7-BdMYB22*, *-WRKY24*, and *-HOS15* was transformed; additionally, *pGADT7-BdHD1* with each of *pGBKT7-BdMYB22*, *-WRKY24*, and *-HOS15* was transformed. A volume of 50 μ L of Y2H Gold (Takara Bio) competent cells were added to the mixture, followed by 500 μ L of PEG/LiAc (8 mL 50% PEG 3350, 1 mL 10x TE buffer, and 1 mL 1M LiAc (10x)). After an incubation period of 30 min at 30 °C 20 μ L of DMSO was added to the mixture. The cells were heat-shocked for 15 min in a 42 °C water bath. The cells were pelleted at 13,000g for 30 seconds and supernatant was discarded. A volume of 1 mL of 0.9% (w/v) NaCl solution (0.9g NaCl in 100 mL ddH₂O) was added to the cells.

For plating of the cells, a volume of 30 μ L of the transformed yeast cells were plated and spread onto Double Dropout medium: SD/-Leu/-Trp (DDO). The cells were incubated at 30 °C for 3-5 days. Colonies were randomly picked from DDO plates after the incubation period and were resuspended in 0.9% (w/v) NaCl solution. The yeast colonies were plated at the default concentration as well as at a 1/10 dilution onto Quadruple Dropout medium: SD/-Leu/-Trp/-His/-Ade (QDO). The formation of colonies was observed after a 3-5 day incubation period at 30 °C. Colonies from the QDO media were then selected and diluted as mentioned above and subsequently plated onto QDO medium supplemented with X- α -Gal and Aureobasidin A (QDO/X/A). After incubation for 3-5 days at 30 °C yeast colony growth was observed. Three technical replications were conducted for each combination of Y2H constructs.

2.10.4 Y2H Experimental Controls

A mixture of the pGADT7-DEST (prey) and the empty pGBKT7 vectors were used for the negative controls for each of the proteins: BdHD1, BdMYB22, BdWRKY24 and BdHOS15. Additionally, *pGBKT7-Lam* and *pGADT7-7* provided in the Y2H kit was used as the negative control, these vectors encode *lamin* and *SV40 large T-antigen*. The positive control from the kit was used: *pGBKT7-53* and *pGADT7-T* which encode *murine p53* and *SV40 large T-antigen*.

2.11 Bimolecular Fluorescence Complementation Assay

Bimolecular fluorescence complementation (BiFC) experiments were carried out to confirm protein-protein interactions (Tian et al., 2011). The coding regions of BdHD1, BdMYB22, BdWRKY24 and BdHOS15 were cloned into both pEarleygate201-YN and pEarleygate202-YC, according to section 2.7. Each of these vectors was separately transferred into *Agrobacterium tumefaciens* (GV3101). *Agrobacterium* was incubated for 2-3 days at 28 °C until colony growth was present on LB medium supplemented with kanamycin and rifamycin.

Fresh colonies for BiFC were prepared by picking single colonies to inoculate 3 mL of LB, containing 50 µg/mL kanamycin (Sigma-Aldrich) and 50 µg/mL rifamycin (Sigma-Aldrich), and grown overnight at 28 °C. Cells were pelleted at 10,000g for 1 min and supernatant was discarded. A volume of 1 mL of infiltration media (5 g/L glucose, 50 mM MES hydrate, 2 mM Na₃PO₄ and 0.1 mM acetosyringone) was added to the pelleted cells and then centrifuged again under the same conditions. Washing of the pellet with the infiltration medium was repeated a total of three times, each time resuspending the pellet in the medium. Cells were finally resuspended in 500 µL infiltration medium. Infiltration medium was added to the cells until the desired OD between 1.0-1.2 was reached. A mixture of *BdHD1-YN* and each of the BdWRKY24, BdMYB22 and BdHOS15 pEarleygate202-YC combinations was created at a 1:1 ratio. Additionally, the mixtures between *BdHD1-YC* and each of the BdWRKY24, BdMYB22 and BdHOS15 pEarleygate201-YN combinations were created as well.

Nicotiana benthamiana plants were grown at 16 h light at 22 °C/8 h dark at 20 °C with 50% humidity. The leaves of five-week-old plants were used for infiltration. The abaxial side of the leaf was infiltrated with 200 µL of the *Agrobacterium* mixture. Each *agrobacterium* mixture was infiltrated into a minimum of two *N. benthamiana* leaves. Infiltrated plants were returned to the same plant growth conditions. After 24-48 hours, the YFP signal was observed using a FV3000 Olympus Confocal Laser Scanning Microscope. The argon excitation laser wavelength was set at 514 nm to visualize the YFP signal. Three technical replicates were conducted for each combination of BiFC constructs.

3 Results

3.1 Identification of Homologous Proteins in *Brachypodium distachyon*

The protein sequence for each candidate interacting *B. distachyon* protein – BdMYB22 (Bradi2g01960), BdWRKY24 (Bradi2g49020), BdWRKY41 (Bradi2g53510), BdHOS15 (Bradi1g52640) and BdPP2C1 (Bradi2g45470) - was acquired from *Phytozome.net*. Using Protein BLAST® (NCBI-National Center for Biotechnology Information, U.S. National Library of Medicine) the corresponding *A. thaliana* proteins homologs were identified for each *B. distachyon* protein. The amino acid sequence alignment between each *B. distachyon* protein and its respective *Arabidopsis* homolog was conducted via Clustal Omega (<https://www.ebi.ac.uk/Tools/msa/clustalo/>).

BdMYB22 shares 79.55% similarity with AtMYB62 (At1g68320) at the protein level (Figure 3.1A). The SANT domain was present in both BdMYB22 and AtMYB62. The SANT domain is a motif related to the MYB DNA-binding domain (Grüne et al., 2003). SANT domain-containing proteins are present in chromatin remodeling enzymes and are known interactors of chromatin modifying complexes involving HDACs (You et al., 2001); therefore BdMYB22 was selected as a candidate interacting protein.

BdWRKY24 is homologous to AtWRKY24 (At5g41570) in *Arabidopsis*; the two proteins share 69.72% similarity (Figure 3.1B). BdWRKY41 shares 30.81% similarity at the protein level with AtWRKY70 (At3g56400) (Figure 3.1C). The WRKY DNA-binding domains were conserved for both BdWRKY24 and BdWRKY41, along with each of their homologous proteins. Additionally, negative regulation of BdWRKY24 by BdHD1 expression in *B. distachyon* was previously identified (Song et al., 2019). Involvement of WRKY transcription factors in gene repression complexes in association with HDACs led to the inclusion of BdWRKY41 to determine potential interactions (Kim et al., 2008).

BdPP2C1 is 53.47% similar to the highly ABA-induced PP2C protein 3 (At2g29380) in *Arabidopsis* (Figure 3.1D). The PP2C domains are involved in dephosphorylation. Dephosphorylation and deacetylation function in unison to mediate gene repression, as observed

(C) BdWRKY41 MQAQSRLMSSAASAADERYEAVVRELRRGHELTAQLQAEARALRGQGQAEATAAFILR
 AtWRKY70 -----MDTNKAKKLVMMNQLVEGHDLTTQLQQLSOPGS--GLEDLVA-----
 :: * : . *

BdWRKY41 EVSRAFTVCISIMGGAAPATPLAEAA-----TAPAGAARRPRDDGAPR-----
 AtWRKY70 KILVCFNNTISVLDTFEPISSSSLAAVEGSQNASCNDNGKFEDSGDSRKRGLGPVKGKRG
 : * . * : : * . * : . * *

BdWRKY41 -----KTIETSSPNSDGYMWRKYGQKRIMKTRFPCRYRCSHHRERGCPATKQVQE
 AtWRKY70 CYKRRKRSETCTIESTILEDASFWRKYGQKEILNAKFRSYPFRCTHKYTQGCKATKQVQK
 . * : . * : * : * : * : * : * : * : * : * : * : * : * : * : * : * : *

BdWRKY41 QQHGDGADHPKTYLVIVVHEHTCRTTPPSAEPEAPVVARGRLARDDDAVPLDGGGGAKE
 AtWRKY70 VE-----LEPKMFSITYIGNHTCNTNAETPKSKTCDH-----HDEIFMDSSEHDKSP
 : * : * : * : * : * : * : * : * : * : * : * : * : * : * : * : *

BdWRKY41 ELERQVLVSSLACVLQGRHTDTTWGGAPAPGAGSSSSSQLGRVSADDAGASASLNALLA
 AtWRKY70 SLS-----TSMKEE-----DNPHRHHGSSTENDLSLVWPEM-----VFE
 . * . : : . * * : * : * : * : * : * : * : * : * : * : * : *

BdWRKY41 TAMPPLTSSLGAGEEEEEELDVMDYDVPADTALCFG-GPSYGMRDDMML*-----
 AtWRKY70 EDY-HHQASYVNGKTSTSIDVLG----SQDLMVFGGGDFEFSENEHFSIFSSCSNLS
 : * * : . : * : * : * : * : * : * : * : * : * : * : * : * : * : *

(D) BdPP2C1 MSTETTSKRDEASLRELLAG-GDKELM--TVARSARRRRLRRLGRTASAAAEEDEGAK
 AtPP2C3 MA-----EIC-YEVVTDACPSVYESTPAHSRRRPRFQ--TVMHE----DWEKNCK
 * : * . * : * : * : * : * : * : * : * : * : * : * : * : * : * : *

BdPP2C1 RVRPAGPLDSCSS--DSSDSAKVTPEPQVPCVSHGAVSVIGRRREMEDAVAVAAPFSAVV
 AtPP2C3 RSKQEALATRYSSIPRSSREDFSDQNVVSPRYGVSSVCGRRREMEDAVAIHPSFSSPK
 * : . * * * * : : . * . *

BdPP2C1 EGDGKEEFFFVYDGHGSRVAEACRERMHVLAEEVQRLRGIQQQRGSGSGRDEEEDVI
 AtPP2C3 N-SEFPQHFGVYDGHGCSHVAARCRERLHKLVEELSSDM-----EDE
 : . : : * . *

BdPP2C1 AGWKEAMAACFARVDGEVVE-----DEAETGEQTVGSTAVVAVGPRRIVVAN
 AtPP2C3 EEWKTTERSFTMRDKEVVSWGDSVVTANCKDLQTPACDSVGSTAVVSVITPDKIVVAN
 * * : * . * : *

BdPP2C1 CGDSRAVLSRAGVPVPLSDDHKPDRPDEMERVEAAGGRVINWNGYRILGVLATRSRIGDY
 AtPP2C3 CGDSRAVLCRNGKPVPLSTDHKPDRPELDRIEGAGGRVIYWDPCRVLGLVAMSRAIGDN
 *

BdPP2C1 YLKPYPVIAEPEVTVMRDTRDKDEFILASDGLWDVVSNEVACKIARNCLSGRAASKYP--E
 AtPP2C3 YLKPYPVSCPEVTITDRRDD-DCLILASDGLWDVVSNETACSVARMCLRGGRRQDNEDP
 *

BdPP2C1 SVSGSTAADAAALLVELAMSRGSKDNISVVVELRRLRSRTAAVIKENRR*
 AtPP2C3 AISDKACTEASVLLTKLALARNSSDNVSVVVIDLRR-----
 : * . . . : * : * : * : * : * : * : * : * : * : * : * : * : * : * : * : *

3.2 Structural Analysis of *B. distachyon* proteins

The protein domains and tertiary structures for each of BdMYB22 (Bradi2g01960), BdWRKY24 (Bradi2g49020), BdWRKY41 (Bradi2g53510), BdHOS15 (Bradi1g52640) and BdPP2C1 (Bradi2g45470) were analyzed using the SMART tool (<http://smart.embl-heidelberg.de/>) and Phyre2 tool (<http://www.sbg.bio.ic.ac.uk/phyre2>), respectively. Protein analysis of BdMYB22 identified two SANT domains (Figure 3.2). This domain is similar to the DNA-binding domain commonly found in members of the MYB superfamily (Boyer et al., 2002). The SANT domain is composed of tandem repeats of three α -helices arranged into helix-turn-helix motifs (Figure 3.3A) (Grüne et al., 2003). Despite the structural similarity between the SANT and MYB domains, the SANT motif is functionally divergent and often found in the chromatin modifying complex (Boyer et al., 2004). Both BdWRKY24 and BdWRKY41 contain the WRKY domain. The WRKY domain forms a four stranded β -sheet containing the WRKYGQK consensus sequence (Eulgem et al., 2000; Yamasaki et al., 2005). WRKY transcription factors bind to DNA to regulate gene expression and are negatively regulated by direct interactions with HDACs (Kim et al., 2008). Analysis of BdHOS15 identified the LisH domain along with 8 WD40 repeats. The LisH (lissencephaly type-1 like homology motif) domain, an α -helix is followed by an uncharacterized coiled-coil region involved in protein dimerization (Gerlitz et al., 2005). The WD40 structural repeats are approximately 40 residues and each form individual blades of the β -propeller domain (Smith et al., 1999). The β -propeller domain provides a surface for the facilitation of protein-protein interactions (Smith et al., 1999). Lastly, BdPP2C1 is characterized by the PP2Cc domain, a serine/threonine phosphatase family 2C catalytic domain. The complex PP2C domain consists of 10 β -strands and 5 α -helices (Smith et al., 1999) and interacts in complexes with HDACs (Canettieri et al., 2003).

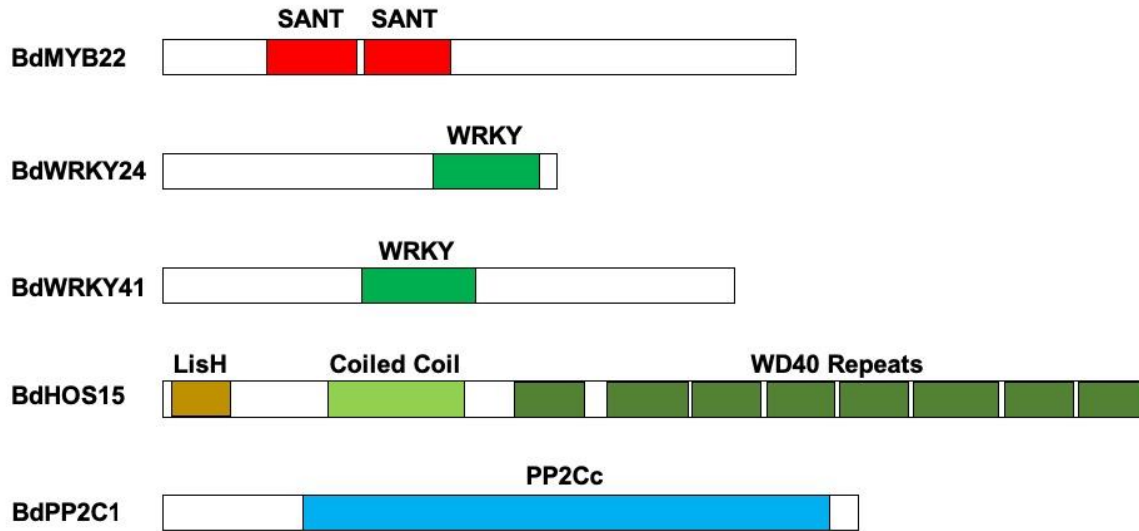


Figure 3.2. Key domains identified in candidate *B. distachyon* proteins.

Key protein domains were predicted for each candidate interacting protein using SMART software (<http://smart.embl-heidelberg.de/>).

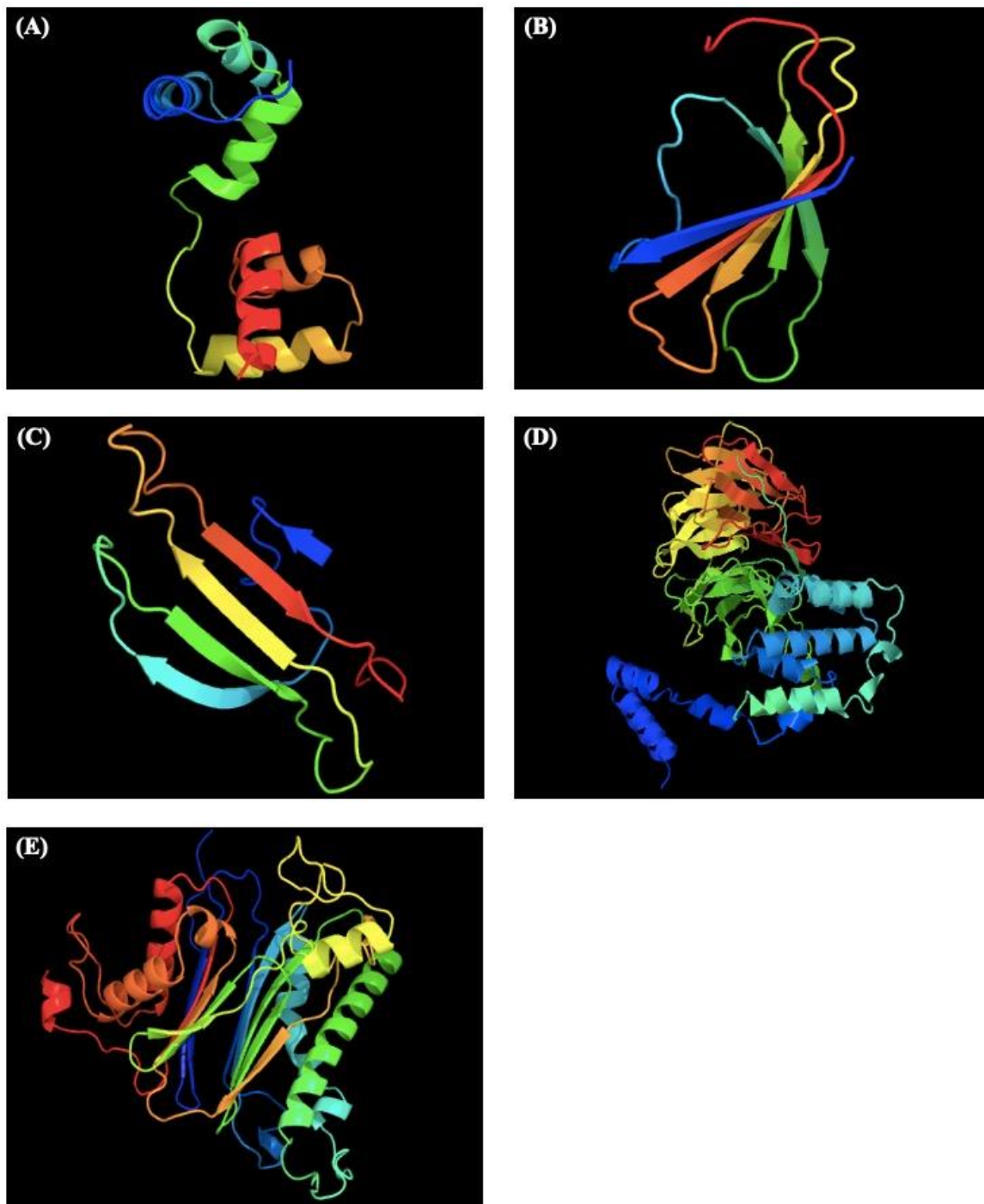


Figure 3.3. Tertiary structures of *Brachypodium distachyon* proteins.

Tertiary structures for the candidate interacting *B. distachyon* proteins were predicted using the Phyre2 tool (<http://www.sbg.bio.ic.ac.uk/phyre2>). Protein structures are shown for (A) BdMYB22, (B) BdWRKY24, (C) BdWRKY41, (D) BdHOS15 and (E) BdPP2C1.

3.3 Gene Cloning of BdMYB22, BdWRKY24 and BdHOS15

Gateway gene cloning was used to amplify the gene coding sequence for each of the candidate genes – BdMYB22, BdWRKY24, BdWRKY41, BdHOS15 and BdPP2C1 – chosen for interaction analysis with BdHD1. Gateway gene cloning utilizes *attB* attachment sequences flanked to the gene coding sequence. Using the gene specific primers, the gene coding regions were amplified and isolated from the wild-type *Brachypodium distachyon* Bd21-3 cDNA. The PCR products were loaded and identified on 1% agarose gels. The correct gene size fragment was obtained for BdMYB22, BdWRKY24 and BdHOS15. Expected band sizes for each of BdMYB22, BdWRKY24 and BdHOS15 were 1074 bp, 669 bp and 1668 bp, respectively (Appendix 1, 2, 4).

Once amplified, the gene coding sequences of BdMYB22, BdWRKY24 and BdHOS15 were inserted into the pDONRTM221 entry vector. The entry vector encodes an antibiotic resistance gene *nptII* which confers resistance to kanamycin; this allows for the selection of transformed *Escherichia coli* cells on the growth medium. The successful recombination of each of these genes was confirmed by single colony PCR using the M13 forward primer and the gene specific reverse primer. The M13 primer sequence is located upstream of the *attP1* site in pDONRTM221 (Figure 3.4A). The correct amplified fragments from the entry vectors with each of BdWRKY24, BdMYB22 and BdHOS15 were identified (Figure 3.4B-D). Once isolated, the identity of the genes BdWRKY24, BdMYB22 and BdHOS15 were confirmed by sequencing analysis.

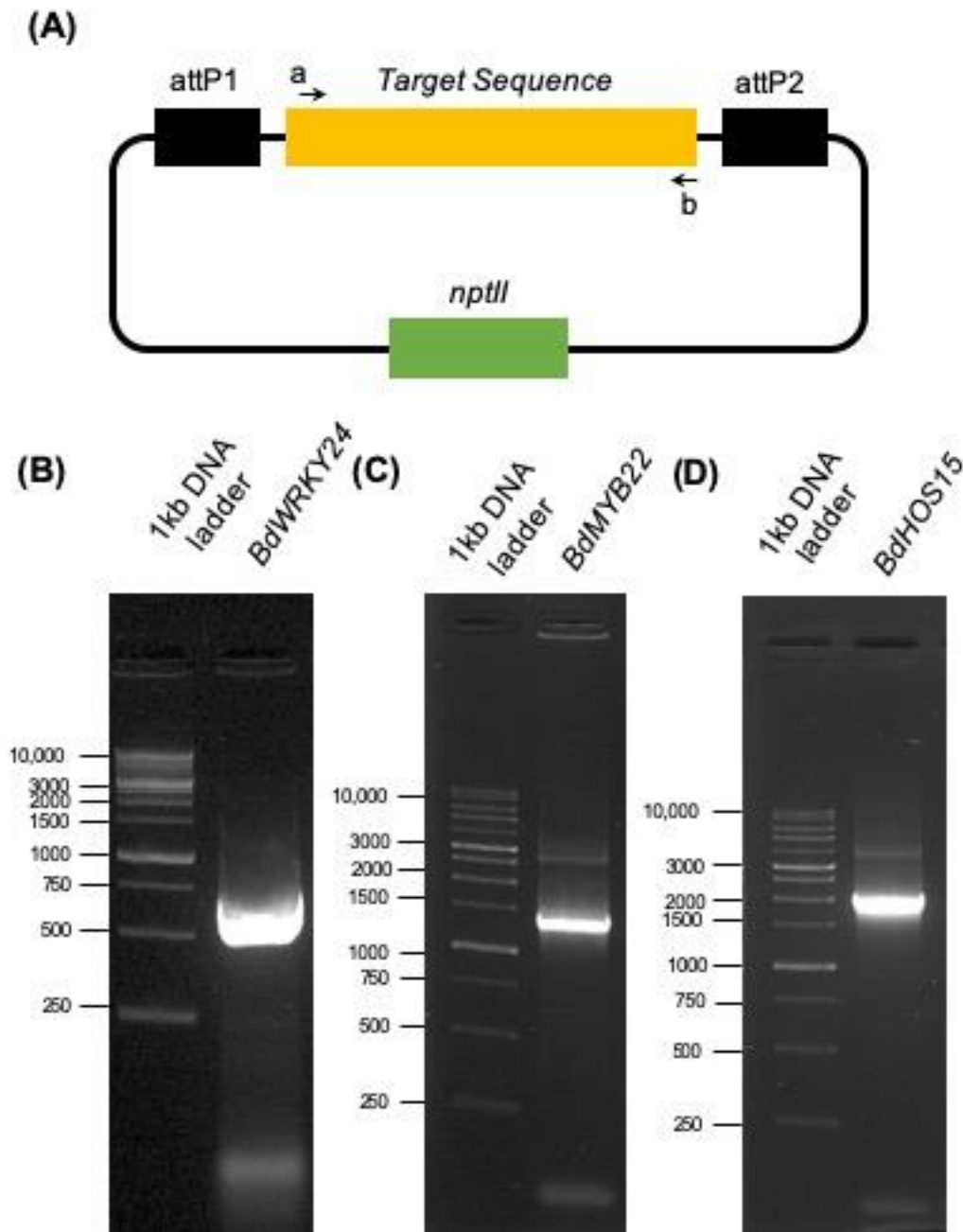


Figure 3.4. Single colony PCR for *pDONR*TM221 constructs.

A, the *pDONR*TM221 entry vector map with primer sites used for single colony PCR. The M13F primer is annotated by a→ and the sequence specific primer is located at the 3' end annotated by ←b. The recombined target sequence is flanked by the *attP1* and *attP2* sites. The *nptII* gene confers resistance to kanamycin. B, the fragment corresponding to *pDONR*TM221-*BdWRKY24* was amplified by using the M13F primer and the *BdWRKY24*-R primer. C, the fragment

corresponding to *pDONRTM221-BdMYB22* was amplified by using the M13F primer and the BdMYB22-R primer. D, the fragment corresponding to *pDONRTM221-BdHOS15* was amplified by using the M13F primer and the BdHOS15-R primer. The correct band size was observed for each gene as each gene was successfully recombined into *pDONRTM221*.

3.4 Cloning of BdWRKY41 and BdPP2C1

The cDNA sequence for BdWRKY41 and BdPP2C1 were not successfully cloned. Gene specific primers with the *attB* attachment sequences were used to isolate the gene coding sequence for each gene. No DNA bands were amplified for neither BdWRKY41 nor BdPP2C1. Gene specific primers without the *attB* attachment sequence were unable to isolate the DNA fragment from the cDNA. Gradient PCR was conducted from 55-65 °C to identify an optimal temperature for amplification, however the correct band size was not identified. The expected sizes of BdWRKY41 and BdPP2C1 were 969 bp and 1179 bp, respectively (Appendix 3 and 5).

3.5 Generation of *pGADT7* and *pGBKT7* Constructs

The destination vectors, *pGADT7* and *pGBKT7*, were required to perform Yeast Two Hybrid (Y2H) experiments. The *pGADT7* vector contains the GAL4 activation domain, whereas the *GBKT7* encodes the DNA-binding domain of GAL4. The coding sequence for each of BdHD1, BdMYB22, BdWRKY24 and BdHOS15 were recombined into the *pGADT7* (prey) and *pGBKT7* (bait) vectors using Gateway® LR Clonase ® (Thermo Fisher Scientific cat. 11791-020) reaction mix. The *pGADT7* and *pGBKT7* constructs used in this experiment contained the *attR1* and *attR2* Gateway® sites for recombination. The *pGADT7* and *pGBKT7* constructs for each of the proteins in this experiment were electroporated into *E. coli* and grown on selective LB medium. The vectors were isolated and assayed for each gene to confirm the integration of the coding sequence into the Y2H constructs.

The constructs were isolated via single colony PCR. The T7-F vector primer and the gene specific reverse primers were used for each vector (Table 2). The T7-F vector primer sequence is located within the T7 promoter upstream of the *attR1* sequence (Figure 3.5A). The correct band size was identified for *pGADT7* constructs for each of BdHD1, BdMYB22, BdWRKY24 and BdHOS15 (Figure 3.5B-E). The fragment sizes were 1634bp, 746bp, 1156bp and 1745bp for

pGADT7-BdHD1, *pGADT7-BdWRKY24*, *pGADT7-MYB22* and *pGADT7-HOS15*, respectively. For all pGBKT7 constructs the correct fragment sizes were identified via single colony PCR (Figure 3.6B-E). The fragment sizes for *pGBKT7-BdHD1*, *pGBKT7-BdWRKY24*, *pGBKT7-BdMYB22* and *pGBKT7-HOS15* were 1638bp, 750 bp, 1160 bp and 1749 bp, respectively.

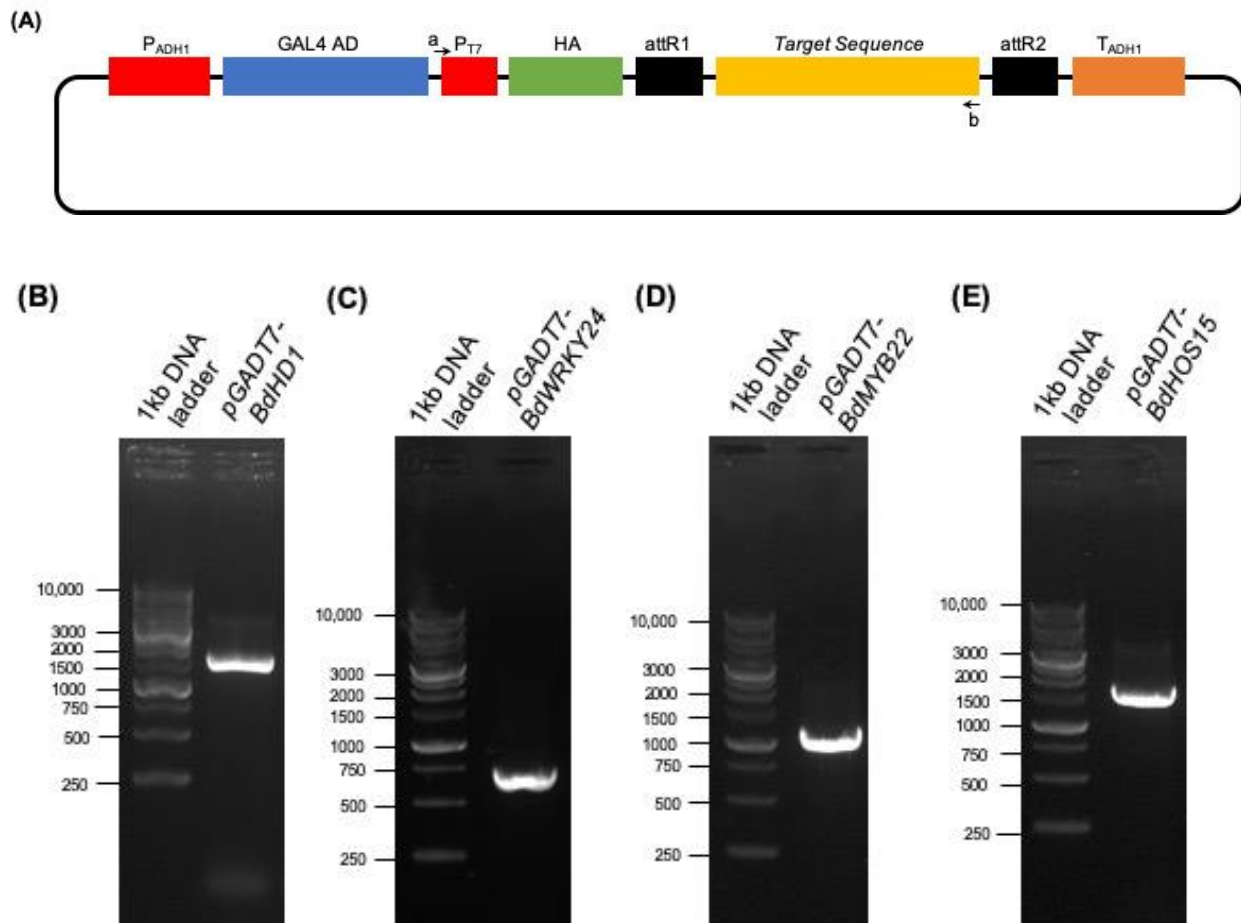


Figure 3.5. Analysis of amplified *pGADT7* destination vector fragments.

A, the *pGADT7* vector map with primer sites used to amplify the recombined genes. The T7-F sequencing primer is annotated by a \rightarrow and the sequence specific primer is located at the 3' end annotated by \leftarrow b. The recombined target sequence is flanked by the *attR1* and *attR2* sites. Other notable features of the vector include: *P_{ADHI}* (*ADHI* promoter), GAL4 activation domain, *P_{T7}* (T7 RNA polymerase promoter), HA tag and *T_{ADHI}* (*ADHI* terminator). B, the fragment corresponding to *pGADT7-BdHD1* was amplified by using the T7-F sequencing primer and the *BdHD1-R* primer. C, the fragment corresponding to *pGADT7-BdWRKY24* was amplified by

using the T7-F sequencing primer and the BdWRKY24-R primer. D, the fragment corresponding to *pGADT7-BdMYB22* was amplified by using the T7-F sequencing primer and the BdMYB22-F primer. E, the fragment corresponding to *pGADT7-BdHOS15* was amplified by using the T7-F sequencing primer and the BdHOS15-R primer. The expected fragment size was observed for all constructs as each gene was successfully recombined into the vector *pGADT7*.

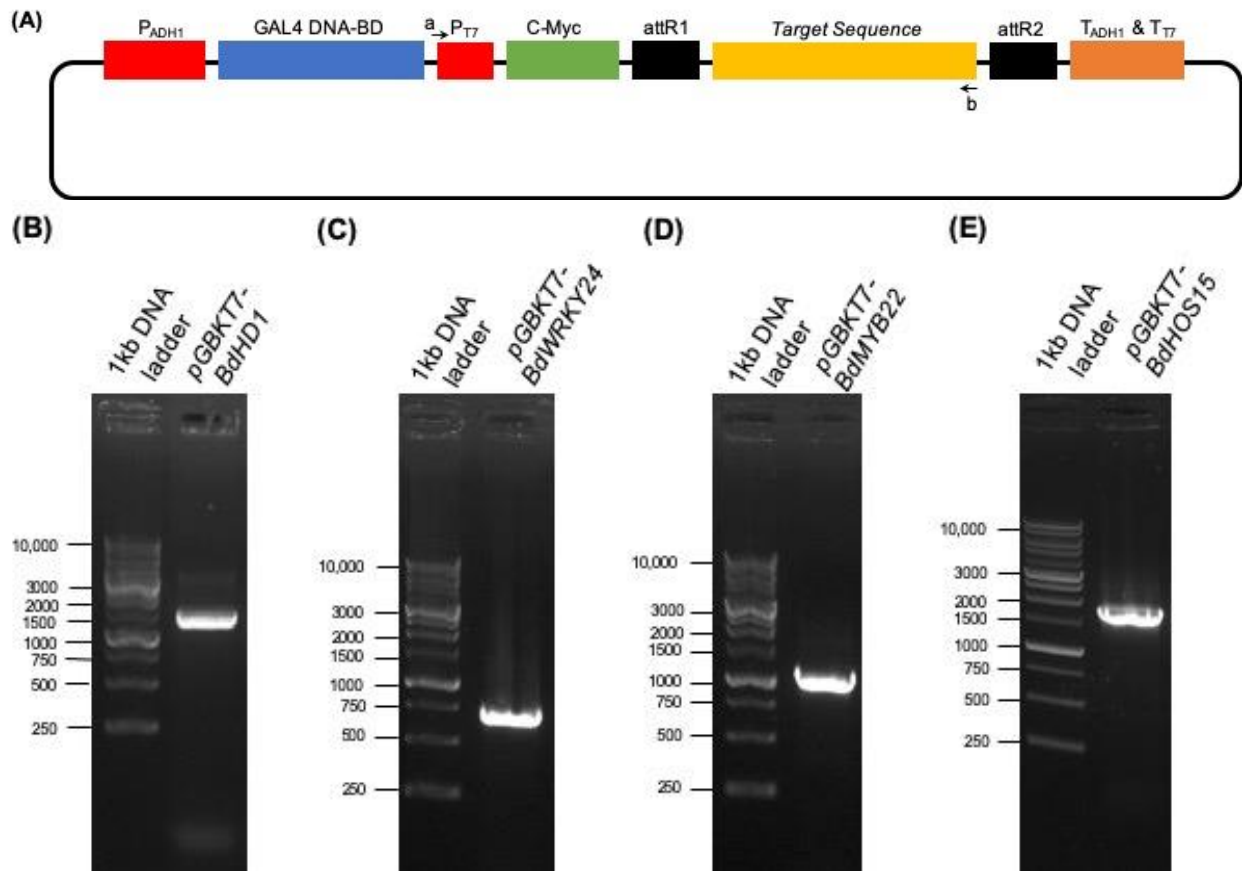


Figure 3.6. Confirmation of *pGBKT7* destination vectors.

A, the *pGBKT7* vector map with primer sites used to amplify the recombined genes. The T7-F sequencing primer is annotated by $a \rightarrow$ and the sequence specific primer is located at the 3' end annotated by $\leftarrow b$. The recombined target sequence is flanked by the *attR1* and *attR2* sites. Other notable features of the vector include: *P_{ADH1}* (*ADH1* promoter), GAL4 DNA-binding domain, *P_{T7}* (T7 RNA polymerase promoter), c-Myc epitope tag, *T_{T7}* (T7 terminator) and *T_{ADH1}* (*ADH1* terminator). B, the fragment corresponding to *pGBKT7-BdHDI1* was amplified by using the T7-F sequencing primer and the BdHDI1-R primer. C, the fragment corresponding to *pGBKT7-BdWRKY24* was amplified by using the T7-F sequencing primer and the BdWRKY24-R primer.

D, the fragment corresponding to *pGBKT7-BdMYB22* was amplified by using the T7-F sequencing primer and the BdMYB22-F primer. E, the fragment corresponding to *pGBKT7-BdHOS15* was amplified by using the T7-F sequencing primer and the BdHOS15-R primer. The expected fragment size was observed for all constructs as each gene was successfully recombined into the vector *pGBKT7*.

3.6 Yeast Two Hybrid (Y2H) Identifies BdHD1 Protein-Protein Interactions

Yeast Two Hybrid (Y2H) was used to identify protein-protein interactions formed between BdHD1 and candidate interacting *B. distachyon* proteins. Y2H is a technology used to screen for protein-protein interactions by screening for physical interactions. The GAL4 protein is cleaved into the GAL4 activation domain and the GAL4 DNA-binding domains. The two vectors used were pGADT7 (prey) and pGBKT7 (bait), which encode the activation and DNA binding domains of GAL4, respectively. The coding sequence of BdHD1 was fused to the GAL4 DNA-binding domain, whereas the coding sequences of each BdMYB22, BdWRKY24, and BdHOS15 were fused to the GAL4 activation domain. Reversibly, BdHD1 also was fused to the activation domain. Meanwhile, BdMYB22, BdWRKY24 and BdHOS15 were fused to the DNA binding domain of GAL4.

S. cerevisiae strain Y2H Gold was transformed with pGBKT7-BdHD1 and each of *pGADT7-BdMYB22*, *pGADT7-WRKY24*, and *pGADT7-HOS15*. Yeast cells were also co-transformed with the reverse constructs: pGADT7-BdHD1 with one of *pGADT7-BdMYB22*, *pGADT7-WRKY24*, and *pGADT7-HOS15*. Each of the co-transformed yeast cells were plated on the Double Dropout (DDO) (-Trp/-Leu) medium. Yeast colonies formed on the DDO medium for all of the bait and prey co-transformations: *pGBKT7-BdHD1 + pGADT7-BdMYB22*, *pGBKT7-BdHD1 + pGADT7-BdWRKY24*, *pGBKT7-BdHD1 + pGADT7-BdHOS15*, *pGBKT7-BdMYB22 + pGADT7-BdHD1*, *pGBKT7-BdWRKY24 + pGADT7-BdHD1* and *pGBKT7-BdHOS15 + pGADT7-BdHD1*. For the both the positive and negative controls, *pGBKT7-53 + pGADT7-T* and *pGBKT7-Lam + pGADT7-7*, respectively, and yeast colony growth was observed on the DDO medium. Growth on the DDO medium indicated successful co-transformation of pGADT7 (bait) and pGBKT7 (prey) constructs into yeast Y2H Gold cells (Figure 3.7a, d, g, j, m, o). The growth on the DDO medium did not indicate whether protein-protein interactions were able to form. Growth on the

DDO medium was consistent across all three experimental repetitions for each co-transformation.

Yeast colonies were picked from the DDO medium and plated onto the Quadruple Dropout (QDO) (-Trp/-Leu/-His/-Ade) medium. Yeast cells co-transformed with *pGBKT7-BdHD1* + *pGADT7-BdMYB22* successfully grew on the QDO medium, indicating that BdHD1 and BdMYB22 are able to interact with each other (Figure 3.7h). Growth on the QDO medium indicates protein-protein interactions via expression of reporter genes HIS3 and ADE2 for histidine and adenine, respectively. Colony formation was observed for both the default concentration and the 1/10 dilution. Likewise, the reverse experiment with the *pGADT7-BdHD1* + *pGBKT7-BdMYB22* constructs resulted in yeast growth on QDO medium (Figure 3.7k). The interaction between BdHD1 and BdMYB22 constructs was consistent for all repetitions on the QDO medium.

The transfer onto the more selective Quadruple Dropout supplemented with X- α -Gal and Aureobasidin A (QDO/X/A) did not yield high quantities of yeast colonies. Growth on QDO/X/A medium confirms the interactions via the expression of additional reporter genes, AUR1-C and MEL1, which encode inositol phosphoryl ceramide synthase and α -galactosidase, respectively. Only colonies containing the *pGADT7-BdHD1* + *pGBKT7-BdMYB22* constructs were able to grow; growth was limited to eight colonies at the default concentration (Figure 3.7l). No colonies were able to grow at the 1/10 dilution or for the reverse experiment with the *pGADT7-BdMYB22* + *pGBKT7-BdHD1* constructs, indicating the interaction is not strong enough to grow on more selective medium (Figure 3.7i).

When cells were co-transformed with *pGBKT7-BdWRKY24* + *pGADT7-BdHD1* and plated onto the QDO medium yeast colony growth was observed at both dilutions, implying that BdHD1 and BdWRKY24 interact with each other (Figure 3.7e). However, no colony growth with the exception of one colony was observed on the QDO medium for the reverse experiments utilizing the *pGBKT7-BdHD1* + *pGADT7-BdWRKY24* constructs (Figure 3.7b). This indicates that the interaction between BdHD1 and BdWRKY24 in the bait and prey constructs is not uniform and may be affected by steric hinderance. The lack of growth on the QDO medium was observed in all experimental repeats, as no colonies were observed in other trials.

The *pGBKT7-BdWRKY24 + pGADT7-BdHD1* co-transformed cells grown on QDO medium were transferred to the QDO/X/A medium. Colony growth was abundant on the QDO/X/A medium at both dilutions, indicating that this interaction between BdHD1 and BdWRKY24 exists (Figure 3.7f). Colony growth on the QDO/X/A medium was observed for all repetitions of the *pGBKT7-BdWRKY24 + pGADT7-BdHD1* co-transformations.

For the experiments involving BdHOS15 and BdHD1 no interaction was observed via the Y2H assays. When transferred to the QDO medium cells with the *pGADT7-BdHD1 + pGBKT7-BdHOS15* or *pGBKT7-BdHD1 + pGADT7-BdHOS15*, no colonies were present (Figure 3.7n, p). In subsequent co-transformations, no colony growth was observed as well. This indicates that BdHD1 and BdHOS15 do not form protein-protein interactions with each other. No cell growth was observed on the QDO/X/A medium as well.

When transferred to the QDO medium, the positive control *pGBKT7-53 + pGADT7-T* grew abundantly at both concentrations. The growth of the positive control also was observed on the QDO/X/A. This indicates that as expected the positive control constructs were able to interact with each other. The negative control provided by the kit, *pGBKT7-Lam + pGADT7-7*, did not grow on either the QDO or QDO/X/A medium. Lastly, the negative controls for each gene used, *pGADT7-BdHD1 + pGBKT7-Empty*, *pGADT7-BdMYB22 + pGBKT7-Empty*, *pGADT7-BdWRKY24 + pGBKT7-Empty*, and *pGADT7-BdHOS15 + pGBKT7-Empty*, were all able to grow on the DDO medium. However, for each of these negative controls no colony growth was observed when transferred to the QDO medium, indicating that the fusion of these proteins to the GAL4 activation domain did not auto-activate reporter gene expression.

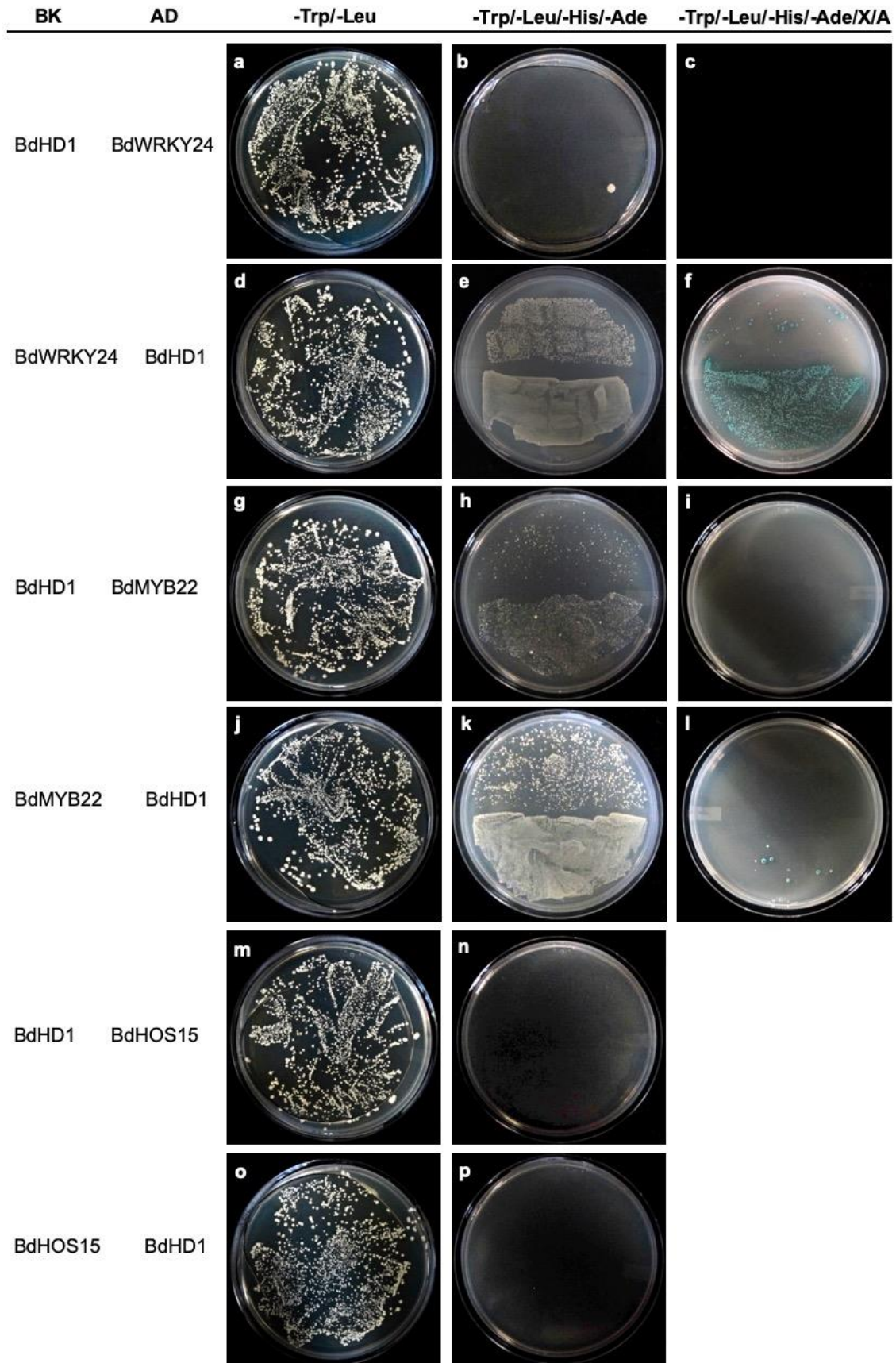


Figure 3.7. BdHD1 in *B. distachyon* interacts with BdMYB22 and BdWRKY24.

Y2HGold yeast strains were plated on either Double Dropout (DDO) (-Trp/-Leu), Quadruple Dropout (QDO) (-Trp/-Leu/-His/-Ade) or Quadruple Dropout supplemented with X- α -Gal and Aureobasidin A (QDO/X/A) medium to determine the ability to grow and identify positive interactions. BK and AD: proteins fused with Gal4 DNA binding and activation domains, respectively. Growth on the DDO medium was observed for each co-transformation of pGBKT7 (bait) and pGADT7 (prey) constructs (a, d, g, j, m, o). Yeast colony growth on the QDO medium identified protein-protein interactions between BdHD1 and each of BdMYB22 and BdWRKY24 (e, h, k). Negligible growth was observed when *pGBKT7-BdHD1* and *pGADT7-BdWRKY24* were co-transformed (b). No growth was observed on QDO medium for co-transformations of BdHD1 with BdHOS1 (n, p). Lastly, confirmation of the protein-protein interaction was conducted using the more selective QDO/X/A medium. Growth on was most abundant on between *pGADT7-BdHD1* and *pGBKT7-BdWRKY24* (f). Little to no growth was observed between BdHD1 and BdMYB22 on the QDO/X/A medium as well as for *pGBKT7-BdHD1* and *pGADT7-BdWRKY24* (c, i, l). These results indicate that BdHD1 interacts strongly with BdWRKY24 and interacts with BdMYB22 as well.

3.7 Construction of *pEarleygate201-YN* and *pEarleygate202-YC* Constructs

To conduct bimolecular fluorescence complementation (BiFC), the coding sequence of each protein in this study was inserted into pEarleygate201-YN and pEarleygate202-YC. The vectors encode either the N- or C-terminal fragment of yellow fluorescent protein (YFP). The coding sequence of each of BdHD1, BdMYB22, BdWRKY24 and BdHOS15 were recombined into the pEarleygate vectors. Vectors were isolated and analyzed from transformed electrocompetent *E. coli* colonies to confirm the transformation.

The pEarleygate vectors were isolated via single colony PCR. The 35SF vector primer and gene specific reverse primers were used to isolate a fragment from the destination vectors (Table 2). The sequence for the 35F vector primer is located within the cauliflower mosaic virus (CaMV) 35S promoter. The promoter is upstream of the 5' end of the transcription initiation site of the inserted gene (Figure 3.8A). The expected band size was identified for pEarleygate201

constructs for each of BdHD1, BdMYB22, BdWRKY24 and BdHOS15 (Figure 3.8B-E). The fragment sizes were 1866 bp, 978 bp, 1383 bp and 1977 bp for *pEarleygate201-BdHD1*, *pEarleygate201-BdWRKY24*, *pEarleygate201-BdMYB22* and *pEarleygate201-BdHOS15*, respectively. The correct fragment size was identified within pEarleygate202-YC destination vectors (Figure 3.9B-E). The expected fragment size corresponding to each vector were 1863 bp, 975 bp, 1380 bp and 1974 bp for *pEarleygate202-BdHD1*, *pEarleygate202-BdWRKY24*, *pEarleygate202-BdMYB22* and *pEarleygate202-BdHOS15*, respectively.

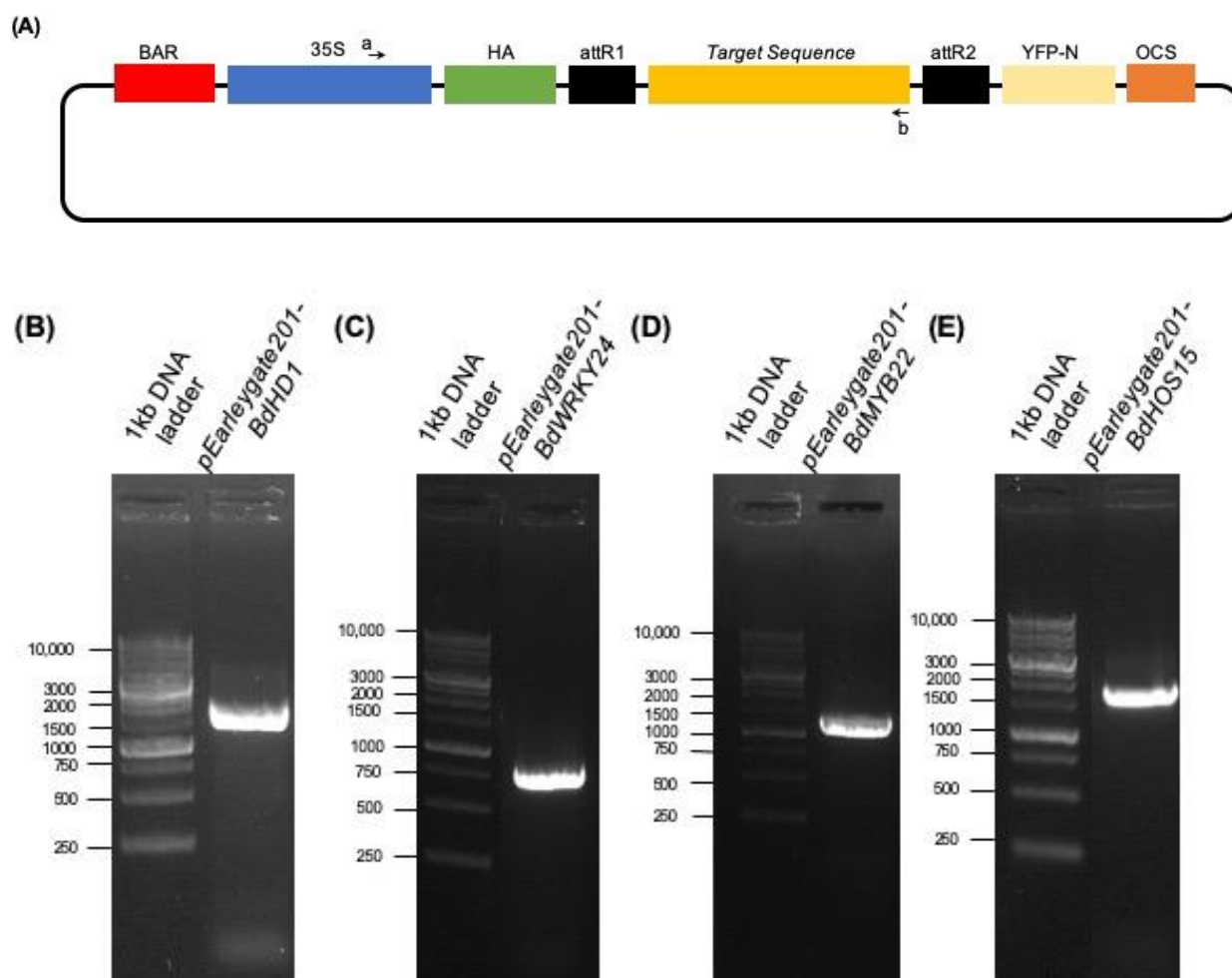


Figure 3.8. Confirmation of *pEarleygate201-YN* destination vectors.

A, the pEarleygate201-YN vector map with primer sites used to amplify the recombined genes. The 35S-F primer is annotated by a→ and the sequence specific primer is located at the 3' end annotated by ←b. The recombined target sequence is flanked by the *attR1* and *attR2* sites. Other

notable features of the vector include: BAR (Basta herbicide resistance gene), 35S (cauliflower mosaic virus 35S promoter), HA tag, YFP-N (yellow fluorescent protein N-terminus) and OCS (3' sequence of octopine synthase gene). B, the proper fragment of *pEarleygate201-BdHHD1* was amplified by using the 35S-F primer and the BdHHD1-R primer. C, the proper fragment of *pEarleygate201-BdWRKY24* was amplified by using the 35S-F primer and the BdWRKY24-R primer. D, the proper fragment of *pEarleygate201-BdMYB22* was amplified by using the 35S-F primer and the BdMYB22-F primer. E, the proper fragment of *pEarleygate201-BdHOS15* was amplified by using the 35S-F sequencing primer and the BdHOS15-R primer. The expected fragment size was observed for all constructs as each gene was successfully recombined into the vector *pEarleygate201-YN*.

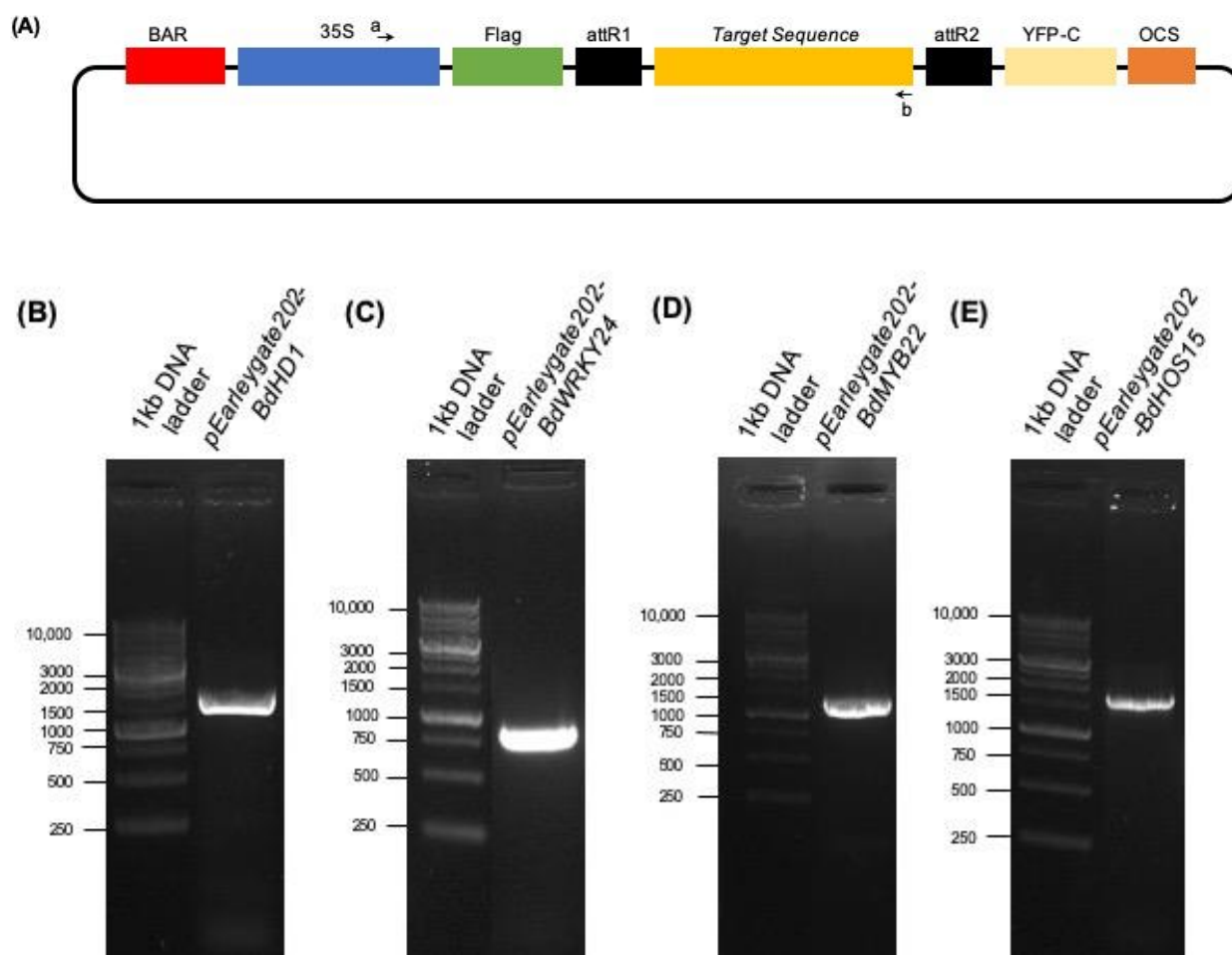


Figure 3.9. Confirmation of *pEarleygate202-YN* destination vectors.

A, the pEarleygate202-YC vector map with primer sites used to amplify the recombined genes. The 35S-F primer is annotated by a → and the sequence specific primer is located at the 3' end annotated by ← b. The recombined target sequence is flanked by the *attR1* and *attR2* sites. Other notable features of the vector include: BAR (Basta herbicide resistance gene), 35S (cauliflower mosaic virus 35S promoter), FLAG tag, YFP-C (yellow fluorescent protein C-terminus) and OCS (3' sequence of octopine synthase gene). B, the proper fragment of *pEarleygate202-BdHD1* was amplified by using the 35S-F primer and the BdHD1-R primer. C, the proper fragment of *pEarleygate202-BdWRKY24* was amplified by using the 35S-F primer and the BdWRKY24-R primer. D, the proper fragment of *pEarleygate202-BdMYB22* was amplified by using the 35S-F primer and the BdMYB22-F primer. E, the proper fragment of *pEarleygate202-BdHOS15* was amplified by using the 35S-F sequencing primer and the BdHOS15-R primer. The expected fragment size was observed for all constructs as each gene was successfully recombined into the vector *pEarleygate202-YC*.

3.8 BiFC confirms interactions between BdHD1 and the transcription factors BdMYB22 and BdWRKY24

The purpose of bimolecular fluorescence complementation (BiFC) was to test and validate the protein-protein interactions identified by the Yeast Two Hybrid Assay. BiFC is a technology used to identify protein-protein interactions *in vivo*. Yellow fluorescent protein (YFP) is used to visualize protein-protein interactions identified via BiFC. YFP is cleaved into two non-overlapping fragments contained within the two vectors used for BiFC, pEarleygate201-YN and pEarleygate202-YC. BiFC was used to confirm the protein-protein interactions between BdHD1 with each BdMYB22, BdWRKY24 and BdHOS15. The coding sequence of BdHD1 was fused to the N-terminus of YFP, meanwhile the coding sequence of BdMYB22, BdWRKY24, and BdHOS15 was fused to the C-terminus of YFP. Reversibly, BdHD1 was fused to the C-terminus and BdMYB22, BdWRKY24, and BdHOS15 were fused to the N-terminus.

The leaves of five-week-old *Nicotiana benthamiana* plants were infiltrated with *BdHD1-YN* and either one of *BdMYB22-YC*, *BdWRKY24-YC*, or *BdHOS15-YC*. Additionally, the leaves were infiltrated with the reverse constructs, using *BdHD1-YC* and one of *BdMYB22-YN*, *BdWRKY24-YN*, or *BdHOS15-YN*. Fluorescence of YFP was observed using the confocal microscope at 526 nm – the excitation wavelength for YFP.

Leaves of *N. benthamiana* co-infiltrated with *BdHDI-YN* and *BdMYB22-YC* expressed the yellow fluorescent signal, indicating protein-protein interactions between these proteins (Figure 3.10d-f). Additionally, the YFP signal was observed when *BdHDI-YC* was co-infiltrated with *BdMYB22-YN* (Figure 3.11d-f). The YFP signal was consistently observed for all repetitions in both construct orientations. The expression of the YFP signal was evident within the nucleus for this interaction. Weaker YFP signals were also present within the cytoplasm and endoplasmic reticulum. The negative controls used were *BdMYB22-YN + Empty-YC* or *Empty-YN + BdMYB22-YC*. For the negative controls, the fluorescent signal was not observed, indicating that the *BdMYB22* BiFC constructs were not auto-fluorescent (Figure 3.10a-c, Figure 3.11a-c).

The co-infiltration of *BdHDI-YN* with *BdWRKY24-YC* in *N. benthamiana* leaves resulted in the expression of YFP, confirming the protein-protein interaction observed via the Y2H assay (Figure 3.10g-i). In reverse experiments with *BdWRKY24-YN* and *BdHDI-YC* constructs, the YFP signal was observable as well (Figure 3.11g-i). The expression of YFP was present within the nucleus for both combinations of constructs. The signal for *BdHDI* with each of *BdWRKY24* was also observable within the cytoplasm and the endoplasmic reticulum. The YFP signal was consistently observable for all experimental repeats of *BdHDI* and *BdWRKY24* co-infiltrations. The negative controls, *BdWRKY24-YN + Empty-YC* and *Empty-YN + BdWRKY24-YC* did not express the YFP signal, indicating no auto-fluorescence.

The co-infiltration between *BdHDI-YN* and *BdHOS15-YC* did not express the YFP signal within *N. benthamiana* leaves, implying that these proteins do not interact with each other (Figure 3.10j-l). No interaction was observed in any experimental repeats with these two constructs. Reverse experiments with *BdHOS15-YN* and *BdHDI-YC* did not yield the YFP signal as well (Figure 3.11j-l). Thus, the lack of signal indicates that there is no interaction, confirming the Y2H assay results. The negative controls for *BdHOS15*, *BdHOS15-YN + Empty-YC* and *Empty-YN + BdHOS15-YC* did not emit the YFP signal. Based on the results of BiFC and Y2H, an interaction between *BdHDI* and *BdHOS15* does not appear to exist.

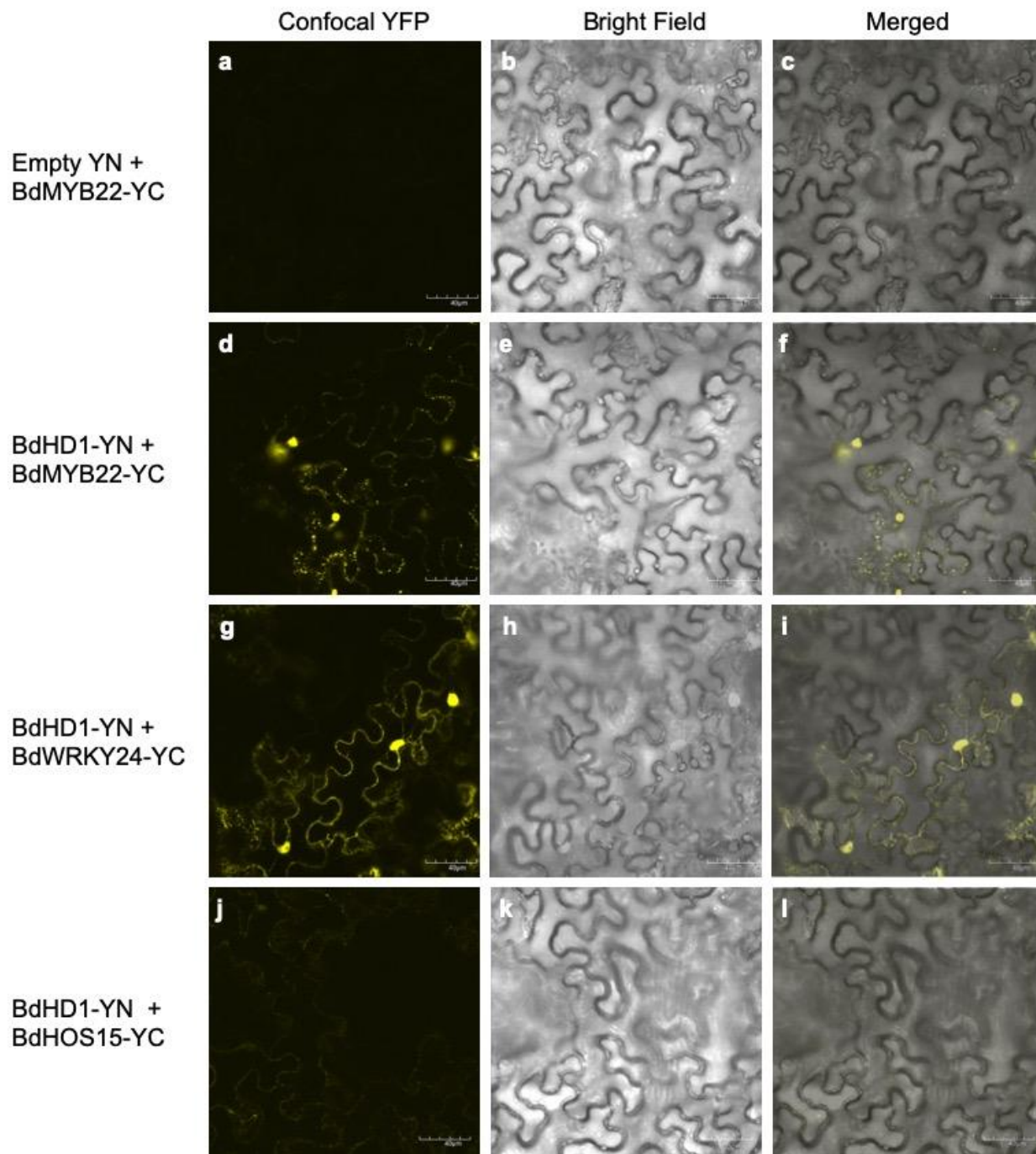


Figure 3.10. BiFC confirms interactions between BdHD1 with each BdMYB22 and BdWRKY24.

BdHD1 fused with the N-terminus of YFP (BdHD1-YN), while BdMYB22, BdWRKY24 and BdHOS15 were fused to the C-terminus of YFP (YC). BdHD1-YN along with each-YC construct were co-infiltrated into leaves of *N. benthamiana*. The leaves were infiltrated using

Agrobacterium tumefaciens and were imaged 48-72 hours after infiltration, using an Olympus confocal microscope. Images are shown as confocal YFP, bright-field or merged confocal YFP + bright-field. Fluorescence was observed between BdHD1 and each of BdMYB22 (d-f) and BdWRKY24 (g-i). No YFP signal was observed in the negative control (a-c) or co-infiltrations between BdHD1 and BdHOS15 (j-l). The interaction between BdHD1 and each of BdMYB22 and BdWRKY24 was confirmed.

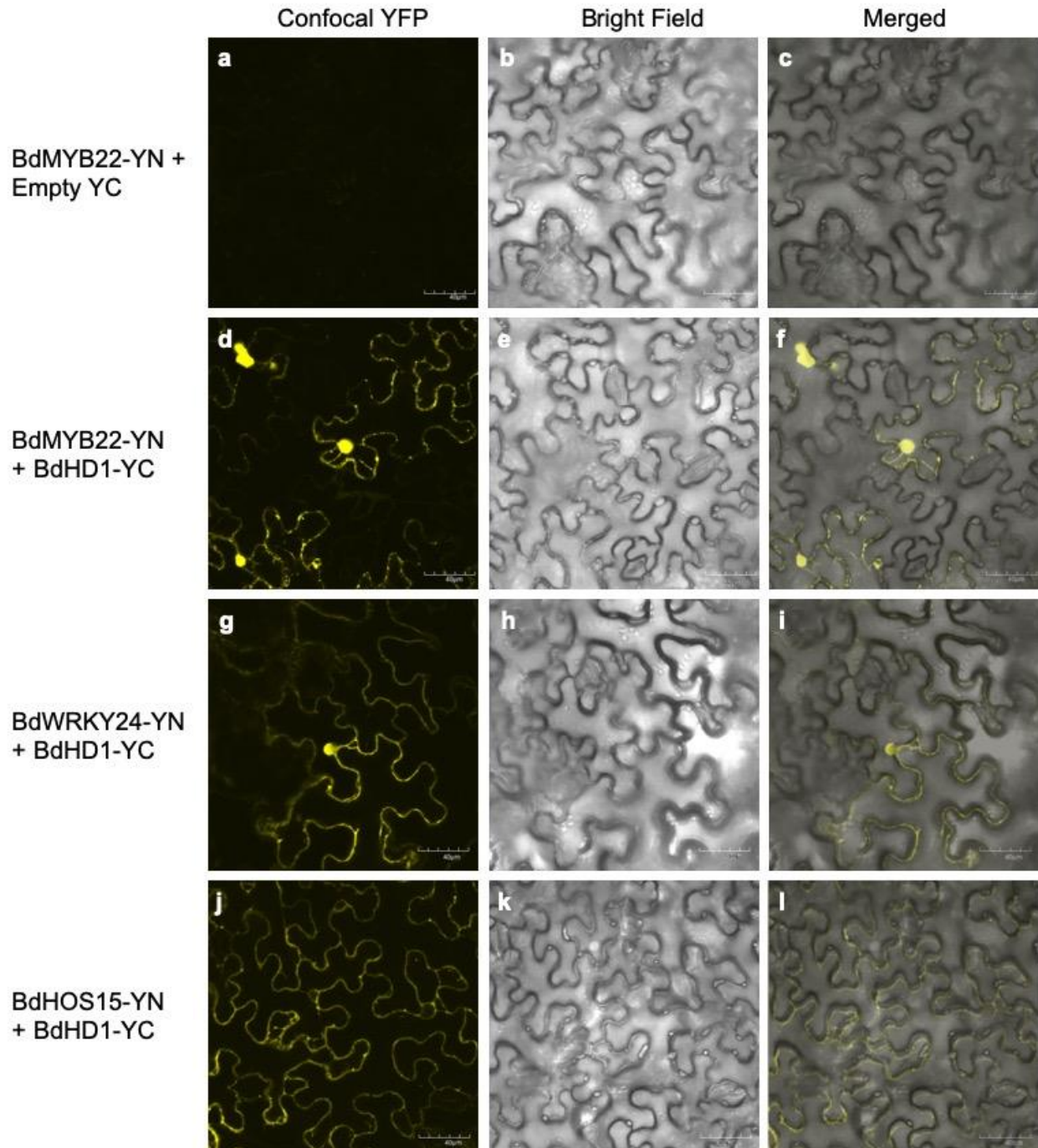


Figure 3.11. BdHD1 interacts with BdMYB22 and BdWRKY24.

BdHD1 fused with the C-terminus of YFP (BdHD1-YC), while BdMYB22, BdWRKY24 and BdHOS15 were fused to the N-terminus of YFP (YN). BdHD1-YC along with each-YN construct were co-infiltrated into leaves of *N. benthamiana*. The leaves were infiltrated using *Agrobacterium tumefaciens* and were imaged 48-72 hours after infiltration, using an Olympus

confocal microscope. Images are shown as confocal YFP, bright-field or merged confocal YFP + bright-field. Fluorescence was observed between BdHD1 and each of BdMYB22 (d-f) and BdWRKY24 (g-i). No YFP signal was observed in the negative control (a-c) or co-infiltrations between BdHD1 and BdHOS15 (j-l). The interaction between BdHD1 and each of BdMYB22 and BdWRKY24 was confirmed.

4 Discussion

4.1 BdHD1 forms protein-protein interactions

The aim of this study was to investigate whether the histone deacetylase BdHD1 found in *Brachypodium distachyon* forms protein-protein interactions. BdHD1 is one of twelve histone deacetylases (HDACs) found within *B. distachyon* (Song et al., 2019). HDACs depress gene regulation by changing the chromatin conformation via histone deacetylation. As previously demonstrated in *Arabidopsis thaliana*, many HDACs do not function individually to alter gene expression (Liu et al., 2014). HDAC protein complexes have been identified in several species, such as *Zea mays* (corn), where a complex involving HDA101 was identified (Yang et al., 2016). The proteins commonly associated with HDACs are typically transcription factors, and they may act to facilitate the specific binding to genes targeted for down-regulation via deacetylation. For example, in *Oryza sativa* (rice), HDA705 interaction assays identified several proteins, including the stress and hormone related transcription factors RSS3, RHSF10 and GAMYB-binding protein (Zhao et al., 2016).

Interactions involving HDACs have been demonstrated in *Arabidopsis*, a model system for dicot plants. Many agriculturally and economically important crops, including wheat, rice, barley and corn, are monocots. In the case of monocot crops, *Arabidopsis* has become an increasingly inapt model, because *Arabidopsis* is both developmentally and physically different. Therefore, *B. distachyon* was selected due to its close ancestry with agriculturally important cereal crops (Opanowicz et al., 2008; Kellogg, 2015). To investigate these interactions, BdHD1, a *B. distachyon* HDAC, was chosen for interaction assays. BdHD1 shares the highest similarity with HDA19 at the protein level. In *Arabidopsis*, HDA19 interactions have been identified (Kim et al., 2008), suggesting that BdHD1 may form interactions in *B. distachyon*.

The current study identified protein-protein interactions between BdHD1 and BdMYB22. The interactions were observed in a yeast system and subsequently confirmed *in vivo* in *Nicotiana benthamiana* by using bimolecular fluorescence complementation (BiFC) assays. The interactions between BdHD1 and BdMYB22 were present in either orientation whether BdMYB22 was fused to the bait or the prey construct. Colony growth was present on QDO plates; however, colony formation was hindered on the more selective QDO/X/A medium. The

interactions appear to not be strong enough to facilitate growth on QDO/X/A, because limited colonies were present on the plates with *pGBKT7-BdMYB* and *pGADT7-BdHD1* constructs. No colonies were present on the plates with *pGBKT7-BdHD1* and *pGADT7-BdMYB22* constructs. Confirmation with BiFC further established the interaction between BdHD1 and BdMYB22. The interactions between these two proteins were localized to the nucleus. The subcellular localization of SANT domain-containing MYB-like transcription factors such as BdMYB22 is generally nuclear (Mott et al., 2003; Zhang et al., 2011). HDACs, including BdHD1, are typically localized to the nucleus (Song et al., 2019), however cytosolic HDAC localization has been observed (De Ruijter et al., 2003). Thus, subcellular localization of this interaction was expected within the nucleus.

The second interaction identified in this study was between BdHD1 and BdWRKY24. This interaction was established with both *in vitro* and *in vivo* systems. The interaction identified between BdHD1 and BdWRKY24 in the Y2H experiments was permutation-dependent. The combination of *pGBKT7-BdWRKY24* (bait) and *pGADT7-BdHD1* (prey) constructs yielded Y2H Gold colonies growing on the QDO and QDO/X/A medium. In experiments using the reciprocal constructs, *pGBKT7-BdHD1* (bait) and *pGADT7-BdWRKY24* (prey), no interaction was detected on either the QDO or the QDO/X/A media. Initially, these results appeared to be contradictory; however, symmetry between interactions is not uniform, because the interactions may be permutation-independent (Brückner et al., 2009). The interactions assayed using the Y2H system may be influenced by the presence of the bait or prey construct, because it may play a role in the ability of the protein to form protein-protein interactions (Brückner et al., 2009).

Mechanistically, steric hinderance may cause these experiments to yield false negatives (Brückner et al., 2009; Galletta and Rusan, 2015). Furthermore, this interaction was observed in BiFC experiments using *N. benthamiana* for both combinations of constructs. The YFP signal was observed when both *BdHD1-YN* and *BdWRKY24-YC* were co-infiltrated into *N. benthamiana*. This result was also observed for the reciprocal experiment with the *BdWRKY24-YN* and *BdHD1-YC* constructs. The interaction between BdHD1 and BdWRKY24 was not permutation dependent in BiFC experiments. The members of the WRKY transcription factor family are localized within the nucleus (Eulgem et al., 2000; Han et al., 2018), hence the interaction with BdHD1 was anticipated within the nucleus. Generally, these results demonstrate that the *B. distachyon* HDAC BdHD1 can interact with each of BdWRKY24 and BdMYB22.

4.2 Interactions between HDACs and MYB-like transcription factors in *Brachypodium distachyon*

An interaction between BdHD1 and MYB-like transcription factor, BdMYB22, was identified in this research. *In silico* analysis of BdMYB22 identified two SANT domains; this domain is related to the MYB DNA binding domain (Codina et al., 2005). The SANT domain is structurally similar to the MYB domain, but alas is functionally divergent, because it does not possess DNA binding capabilities (Boyer et al., 2002). Unlike the MYB domain, the surface of the SANT domain is negatively charged, thus rendering any interaction with the negatively charged DNA backbone highly unlikely (Grüne et al., 2003). This domain interestingly is typically found within multiple chromatin modifying complexes in association with HDAC proteins (Boyer et al., 2002).

In *B. distachyon*, BdHD1 is involved in the deacetylation of H3K9 (Song et al., 2019). The chromatin structure is linked to post-translational modifications, including histone deacetylation (Garcia-Ramirez et al., 1995). The SANT domain is present in several chromatin modifying enzymes, including SWI/SNF COMPLEX SUBUNIT SWI3 (SWI3), TRANSCRIPTIONAL ADAPTOR 3 (ADA3), NUCLEAR RECEPTOR COREPRESSOR (N-CoR), and TRANSCRIPTION FACTOR III B (TFIIB) (Boyer et al., 2002). The SANT domain facilitates HDAC activity via recognition and binding of the histone tail (Boyer et al., 2002). Thus, an interaction between BdHD1 and BdMYB22 was anticipated due to the SANT domains present in BdMYB22. This role in chromatin modifying complexes is observed across eukaryotic systems (Boyer et al., 2004).

Several key enzymes involved in chromatin modifying complexes contain the SANT domain and form protein-protein interactions with HDACs. In human HeLa cells, the co-purification of HDAC1 and HDAC2 complexes identified CoREST and MTA-1 as interacting members (Humphrey et al., 2001). The SANT domain was identified within these key proteins through structural analysis (Humphrey et al., 2001). The SANT domain is essential for the activity of these enzymes, because the removal of the SANT domain in CoREST not only eliminated the CoREST-HDAC1 interaction, but HDAC activity as well (You et al., 2001). Additionally, the co-repressors SMRT and NCoR are both SANT domain-containing proteins identified within HDAC interacting complexes (Andres et al., 1999; Yu et al., 2003). In *Drosophila*, ISWI is a

nucleosome remodeling ATPase encoding a C-terminal SANT domain and N-terminal ATPase region (Grüne et al., 2003). The SANT domain is critical for binding to the histone, enabling the ATPase region to alter the histone-DNA interaction (Grüne et al., 2003). Overall, a well-established link exists between SANT domain-containing enzymes and proper substrate recognition for chromatin modifying proteins.

The SANT domain and interactions between HDAC and SANT domain-containing proteins has been reported in plant systems including *Arabidopsis*. A complex involving POWERDRESS (PWR) and HDA9 that regulates gene expression in aging has been identified in *Arabidopsis* (Chen et al., 2016). PWR is a SANT domain-containing protein that directly binds with HDA9 to repress the expression of targeted genes (Mayer et al., 2019). Histone deacetylation depends on the presence and interaction of PWR with HDA9, because in *pwr* mutant lines, histone acetylation was increased at target genes (Chen et al., 2016). This illustrates the involvement of SANT domain-containing proteins and HDACs as regulators of gene expression via chromatin remodeling.

Based on the observations of this study in combination with previous research, interactions between SANT domain-containing proteins and HDACs are conserved across different organisms. The interaction between the *B. distachyon* proteins BdHD1 and BdMYB22 suggests these proteins are involved in chromatin modifying complexes of monocot cereal crops. It seems plausible that BdMYB22 may be key to targeting the deacetylase activity of BdHD1 to appropriate genes. However, the binding of SANT domain-containing proteins to HDACs does not imply its role in activation of the HDACs' function. For example, SMRT, a SANT domain-containing protein, is able to bind with each of HDAC3 and HDAC4 (Guenther et al., 2002). However, upon further analysis, only the interaction between HDAC3 and SMRT was able to activate the deacetylase activity of HDAC3 (Guenther et al., 2002). Thus, additional experiments are necessary to fully understand the role of BdMYB22 and other potential SANT domain-containing proteins on HDAC activity in *B. distachyon*.

4.3 Interactions between HDACs and WRKY transcription factors in *B. distachyon*

BdWRKY24 and BdWRKY41 are both members of the WRKY transcription factor family. The WRKY family is plant-specific and among the largest transcription factor families (Rushton et al., 2010). A total of 72 and 86 WRKY transcription factors have been identified in *Arabidopsis* and *B. distachyon*, respectively (Eulgem and Somssich, 2007; Tripathi et al., 2012). Members of this family were primarily identified in pathogen defense signaling pathways. The involvement of WRKY in plant abiotic stress-responses has been demonstrated. WRKY proteins regulate gene expression in response to abiotic stresses including heat, cold and drought-stress (Qiu and Yu, 2009).

The WRKY domain was identified in the *B. distachyon* proteins BdWRKY24 and BdWRKY41. Further analysis identified BdWRKY24 as a homologous partner of AtWRKY24 in *Arabidopsis*. Additionally, BdWRKY41 shared the highest similarity at the protein level with AtWRKY70. AtWRKY24 belongs to group IIc, because it possess a single WRKY domain and the C₂H₂ zinc finger motif (Eulgem et al., 2000). Similarly, BdWRKY24 was classified as a member of group IIc. Conversely, AtWRKY70 contains one WRKY domain, but is classified as group III on the basis of the C₂-HC zinc-finger-like motif; as expected BdWRKY41 is a member of group III.

The interaction between BdHD1 and BdWRKY24 is remarkable, because the expression of *BdWRKY24* is sensitive to BdHD1 under drought stress conditions (Song et al., 2019). In wild-type *B. distachyon* plants, BdWRKY24 expression is up-regulated under drought stress, however the expression of *BdWRKY24* was repressed in the *BdHD1*-overexpression lines (Song et al., 2019). In *Arabidopsis*, no current experiments have investigated any interactions between AtWRKY24 specifically with HDAC proteins. This interaction demonstrates the ability of BdHD1 and BdWRKY24 to form protein-protein interactions with each other.

Both WRKY transcription factors and HDACs are known to form protein-protein interactions, therefore it is important to map out interactions between these protein families to gain insight to the HDAC-complex in plants. Interactions between WRKY and HDACs have been observed within the dicot model system *Arabidopsis*. In *Arabidopsis*, HDA19 interacts with each of AtWRKY38 and AtWRKY62 to negatively regulate downstream transcriptional activity of the

WRKY proteins (Kim et al., 2008). More recently, a complex involving interactions between HDA9, AtWRKY53 and POWERDRESS was identified in *Arabidopsis* (Chen et al., 2016). This research has observed an interaction between BdHD1 and BdWRKY24, suggesting BdHD1 may act with BdWRKY24 to regulate gene expression. Interactions between WRKY and HDAC proteins may provide a mechanism by which plants facilitate gene regulation in response to abiotic stress. Further research and identification of other interacting WRKY proteins in *B. distachyon* may lead to further insight into stress response in monocot crops.

Because BdWRKY41 was not successfully cloned, interaction studies between BdHD1 and BdWRKY41 were not assayed. Based on research conducted on AtWRKY70 in *Arabidopsis*, it is possible that an interaction is present, because both are involved in regulating gene expression in drought stress-response. Initially, AtWRKY70 had been identified to regulate plant defense response to biotic stress, in addition to osmotic stress, in *Arabidopsis* (Li et al., 2004, 2013). In *wrky70* and *wrky54wrky70*, mutant line tolerance to osmotic stress was increased relative to wild-type plants; the tolerance was stronger in the double mutant (Li et al., 2013). Thus, AtWRKY70 and AtWRKY54 act together to negatively co-regulate ABA-dependent stomatal closure in response to osmotic stress (Li et al., 2013). Additional roles in brassinosteroid (BR)-regulated plant growth along with drought stress have been identified for AtWRKY70 (Chen et al., 2017). AtWRKY70 interacts with BRASSINOSTEROID INSENSITIVE1-EMS-SUPPRESSOR1 (BES1) to induce the expression of BR-regulated plant growth genes, while repressing drought-responsive gene expression under normal conditions (Chen et al., 2017). Under drought stress, BR-INSENSITIVE2 (BIN2) phosphorylation of AtWRKY70 decreased the protein stability of AtWRKY70, increasing the expression of drought responsive genes (Chen et al., 2017). Given that the closest homolog of BdWRKY41 plays a role in drought response in *Arabidopsis*, an interaction with the drought responsive BdHD1 is a possibility, especially with knowledge of a previous interaction with BdWRKY24.

4.4 No interaction between BdHD1 and BdHOS15 observed

This study did not identify a protein-protein interaction between BdHD1 and BdHOS15 via the Y2H and BiFC assays. In *Arabidopsis*, HIGH EXPRESSION OF OSMOTICALLY RESPONSIVE GENE15 (HOS15) is a transcriptional co-repressor involved in flowering and cold stress response (Zhu et al., 2008). The protein assayed in this study, BdHOS15, shares

58.56% sequence similarity with AtHOS15 at the protein level. AtHOS15 is able to form physical interactions with histone H4, as well as with histone deacetylase HDA9 (Zhu et al., 2008; Park et al., 2019).

AtHOS15 associates with HDAC complexes to repress the expression of downstream stress-related genes (Park et al., 2019). AtHOS15 is a negative regulator of stress response, as exhibited by the increased expression of the stress responsive genes COR15A and ADH1 in *hos15* mutant lines (Zhu et al., 2008). The interaction between HDAC9 and AtHOS15 is required for appropriate gene expression (Park et al., 2019). In *hda9-1* transgenic plants, HDA9 and AtHOS15 are unable to form the HDAC complex, resulting in reduced binding of the GIGANTEA (GI) promoter (Park et al., 2019). This ultimately results in the increased expression of downstream cold-induced genes (Park et al., 2019). Recent research involving the HOS15 and HDA9 complex has identified the SANT domain-containing protein POWERDRESS (PWR) as a component of the complex (Mayer et al., 2019). Additional HDAC complexes involving AtHOS15 have been reported in *Arabidopsis*, including HD2C (Park et al., 2018a) and HDA19 (Mayer et al., 2019).

The interaction between AtHOS15 with HDA19 was identified and confirmed using both Co-immunoprecipitation (Co-IP) experiments and luciferase complementation imaging (LCI) assays (Park et al., 2018b). As previously stated, AtHOS15 is highly similar at the protein level to BdHOS15 found in *B. distachyon*. BdHD1 was reported to share 78.2% similarity at the protein level with HDA19 (Song et al., 2019), therefore an interaction between BdHD1 and BdHOS15 was expected. However, these proteins did not interact in either the Y2H or BiFC assays. Although BdHD1 and BdHOS15 did not interact, it is still possible that an interaction exists between HDACs and BdHOS15 in *B. distachyon*. The LisH domain and WD-40 repeats were identified within BdHOS15. The lissencephaly type-1 like homology motif (LisH) is an α -helical domain involved in the dimerization of AtHOS15 (Gerlitz et al., 2005). The identified WD40 repeats are structural repeats forming a stable β -propeller to facilitate the formation of protein complexes (Smith et al., 1999; Mascheretti et al., 2013). Therefore, due to the presence of these essential motifs in BdHOS15, it is still likely to be involved in HDAC complex formation in *B. distachyon*. *Bradi5g09190* encodes BdHD9, which shares 88.3% similarity at the protein level

with HDA9, thus perhaps providing a stronger potential interacting partner with BdHOS15 (*Phytozome.net*).

5 Future Perspectives

This study reported protein-protein interactions between the *Brachypodium distachyon* histone deacetylase BdHD1, and each of BdMYB22 and BdWRKY24. In *B. distachyon*, BdHD1 is the closest homologous gene to HDA19 from *Arabidopsis thaliana* (Song et al., 2019). Previous research identified AtHDA19 protein-protein interactions to form functional repressor complexes (Gonzalez et al., 2007; Kim et al., 2008; Park et al., 2018b). Based on this knowledge, it is possible that interactions between BdHD1 and each of BdMYB22 and BdWRKY24 may be involved in regulating gene expression.

In *B. distachyon*, BdHD1 plays a role in the positive regulation of drought response (Song et al., 2019). Previous studies identified BdWRKY24 as responsive to drought stress and sensitive to changes in BdHD1 expression (Song et al., 2019). The gene expression of BdMYB22 under drought stress conditions has not been quantified. Future research may assess the drought responsiveness of BdMYB22. The SANT domain present within BdMYB22 is associated with histone chromatin modifying complexes to couple HDAC activity to the histone tail (Boyer et al., 2002). Assessment of the BdMYB22's sensitivity to drought stress may provide a mechanism for the observed interaction in this study. To be able to fully establish the roles of BdWRKY24 and BdMYB22 in *B. distachyon*, it is necessary to perform functional gene analysis of each protein.

Two of the five candidate interacting proteins, BdWRKY41 and BdPP2C1, were not cloned in this study and therefore no interaction studies were conducted. To successfully clone these proteins and determine whether BdHD1 can interact with either of these proteins would be an interesting objective for future studies. In *Arabidopsis*, AtWRKY70 interacts with AtHDA19 under drought stress (Chen et al., 2017), and both are homologous genes of BdWRKY41 and BdHD1. An interaction in *B. distachyon* would suggest some HDAC protein-protein interactions may be conserved between monocots and dicots to regulate abiotic stress. PP2C1 is a serine/threonine protein phosphatase in *B. distachyon*. The activity and interaction of protein phosphatases with HDACs to regulate expression is evident within *Arabidopsis* (Wera and Hemmingst, 1995). The identification of this interaction would suggest that dephosphorylation

and histone deacetylation by BdPP2C1 and BdHD1, respectively, may act in unison to repress gene expression in *B. distachyon* (Canettieri et al., 2003). Regardless of this limitation of the study, the identified interactions with BdHD1 provide a gateway for the continued identification of interacting partners in BdHD1-complexes in *B. distachyon*.

References

- Abe, H., Yamaguchi-shinozaki, K., Urao, T., and Hosokawa, C.D.** (1997). Role of Arabidopsis MYC and MYB Homologs in Drought- and Abscisic Acid-Regulated Gene Expression. *Plant Cell* **9**: 1859–1869.
- Alinsug, M. V., Chen, F.F., Luo, M., Tai, R., Jiang, L., and Wu, K.** (2012). Subcellular localization of class II HDAs in *Arabidopsis thaliana*: Nucleocytoplasmic shuttling of HDA15 is driven by light. *PLoS One* **7**: 1–14.
- Allfrey, V., Faulkner, R., and Mirsky, A.E.** (1964). Acetylation and methylation of histones and their possible role in the regulation of RNA synthesis. *Proc. Natl. Acad. Sci.* **51**: 786–94.
- Anderson, J.D., Lowary, P.T., and Widom, J.** (2001). Effects of histone acetylation on the equilibrium accessibility of nucleosomal DNA target sites. *J. Mol. Biol.* **307**: 977–985.
- Andres, M.E., Burger, C., Peral-Rubio, M.J., Battaglioli, E., Anderson, M.E., Grimes, J., Dallman, J., Ballas, N., and Mandel, G.** (1999). CoREST: A functional corepressor required for regulation of neural-specific gene expression. *Proc. Natl. Acad. Sci.* **96**: 9873–9878.
- Avvakumov, N. and Cote, J.** (2007). The MYST family of histone acetyltransferases and their intimate links to cancer. *Oncogene* **26**: 5395–5407.
- Benhamed, M., Bertrand, C., Servet, C., and Zhou, D.-X.** (2006). Arabidopsis GCN5, HD1, and TAF1/HAF2 interact to regulate histone acetylation required for light-responsive gene expression. *Plant Cell* **18**: 2893–2903.
- Berger, S.L.** (2007). The complex language of chromatin regulation during transcription. *Nature* **447**: 407–412.
- Boyer, L.A., Langer, M.R., Crowley, K.A., Tan, S., Denu, J.M., and Peterson, C.L.** (2002). Essential Role for the SANT Domain Chromatin Remodeling Enzymes. *Mol. Cell* **10**: 935–

942.

- Boyer, L.A., Latek, R.R., and Peterson, C.L.** (2004). The SANT domain: A unique histone-tail-binding module? *Nat. Rev. Mol. Cell Biol.* **5**: 158–163.
- Brownell, J.E. and Allis, C.D.** (1996). Linking histone acetylation to chromatin assembly and gene activation. *Curr. Opin. Genet. Dev.* **6**: 176–184.
- Brückner, A., Polge, C., Lentze, N., Auerbach, D., and Schlattner, U.** (2009). Yeast two-hybrid, a powerful tool for systems biology. *Int. J. Mol. Sci.* **10**: 2763–2788.
- Buszewicz, D. et al.** (2016). HD2C histone deacetylase and a SWI/SNF chromatin remodelling complex interact and both are involved in mediating the heat stress response in *Arabidopsis*. *Plant Cell Environ.* **39**: 2108–2122.
- Camporeale, G., Oommen, A.M., Griffin, J.B., Sarath, G., and Zemleni, J.** (2007). K12-biotinylated histone H4 marks heterochromatin in human lymphoblastoma cells. *J. Nutr. Biochem.* **18**: 760–768.
- Canettieri, G., Morantte, I., Guzmán, E., Asahara, H., Herzig, S., Anderson, S.D., Iii, J.R.Y., and Montminy, M.** (2003). Attenuation of a phosphorylation-dependent activator by an HDAC – PP1 complex. *Nat. Struct. Biol.* **10**: 175–181.
- Chen, J., Yin, Y., Nolan, T., Xin, P., Li, Z., Ye, H., Chu, J., Zhang, M., Chu, C., and Tong, H.** (2017). *Arabidopsis* WRKY46, WRKY54 and WRKY70 Transcription Factors Are Involved in Brassinosteroid-Regulated Plant Growth and Drought Response. *Plant Cell* **29**: 1425–1439.
- Chen, L. and Wu, K.** (2010). Role of histone deacetylases HDA6 and HDA19 in ABA and abiotic stress response. *Plant Signal. Behav.* **5**: 1318–1320.
- Chen, L.T., Luo, M., Wang, Y.Y., and Wu, K.** (2010). Involvement of *Arabidopsis* histone deacetylase HDA6 in ABA and salt stress response. *J. Exp. Bot.* **61**: 3345–3353.
- Chen, X., Lu, L., Mayer, K.S., Scalf, M., Qian, S., Lomax, A., Smith, L.M., and Zhong, X.**

- (2016). POWERDRESS interacts with HISTONE DEACETYLASE 9 to promote aging in Arabidopsis. *Elife* **5**: 1–23.
- Chien, C.T., Bartel, P.L., Sternglanz, R., and Fields, S.** (1991). The two-hybrid system: a method to identify and clone genes for proteins that interact with a protein of interest. *Proc. Natl. Acad. Sci.* **88**: 9578–9582.
- Chinnusamy, V. and Zhu, J.K.** (2009). Epigenetic regulation of stress responses in plants. *Curr. Opin. Plant Biol.* **12**: 133–139.
- Choudhary, C., Kumar, C., Gnad, F., Nielsen, M.L., Rehman, M., Walther, T.C., Olsen, J. V, and Mann, M.** (2009). Lysine acetylation targets protein complexes and co-regulates major cellular functions. *Science* **325**: 834–40.
- Codina, A., Love, J.D., Li, Y., Lazar, M.A., Neuhaus, D., and Schwabe, J.W.R.** (2005). Structural insights into the interaction and activation of histone deacetylase 3 by nuclear receptor corepressors. *Proc. Natl. Acad. Sci.* **102**: 6009–6014.
- Cominelli, E. et al.** (2005). A Guard-Cell-Specific MYB Transcription Factor Regulates Stomatal Movements and Plant Drought Tolerance. *Curr. Biol.* **15**: 1196–1200.
- Dai, X., Wang, Y., Yang, A., and Zhang, W.** (2012). OsMYB2P-1, an R2R3 MYB Transcription Factor, Is Involved in the Regulation of Phosphate-Starvation Responses and Root Architecture in Rice. *Plant Physiol.* **159**: 169–183.
- Deng, W., Liu, C., Pei, Y., Deng, X., Niu, L., and Cao, X.** (2007). Involvement of the Histone Acetyltransferase AtHAC1 in the Regulation of Flowering Time via Repression of FLOWERING LOCUS C in Arabidopsis. *Plant Physiol.* **143**: 1660–1668.
- Devoto, A., Nieto-rostro, M., Xie, D., Ellis, C., Harmston, R., Patrick, E., Davis, J., Sherratt, L., Coleman, M., and Turner, J.G.** (2002). COI1 links jasmonate signalling and fertility to the SCF ubiquitin–ligase complex in Arabidopsis. *Plant J.* **32**: 457–466.
- Draper, J., Mur, L.A.J., Jenkins, G., Ghosh-Biswas, G.C., Bablak, P., Hasterok, R., and Routledge, A.P.M.** (2001). *Brachypodium distachyon*. A New Model System for

Functional Genomics in Grasses. *Plant Physiol.* **127**: 1539–1555.

- Dubos, C., Stracke, R., Grotewold, E., Weisshaar, B., and Martin, C.** (2010). MYB transcription factors in Arabidopsis. *Trends Plant Sci.* **15**: 573–581.
- Dutnall, R.N., Tafrov, S.T., Sternglanz, R., and Ramakrishnan, V.** (1998). Structure of the Histone Acetyltransferase Hat1: A Paradigm for the GCN5-Related N-acetyltransferase Superfamily. *Cell* **94**: 427–438.
- Earley, K.W., Haag, J.R., Pontes, O., Opper, K., Juehne, T., Song, K., and Pikaard, C.S.** (2006). Gateway-compatible vectors for plant functional genomics and proteomics. *Plant J.* **45**: 616–629.
- Eom, G.H., Cho, Y.K., Ko, J., Shin, S., Phosphorylates, C.K., and Hdac, S.** (2011). Casein Kinase-2 α 1 Induces Hypertrophic Response by Phosphorylation of Histone Deacetylase 2 S394 and its Activation in the Heart. *Circulation* **123**: 2392–2403.
- Eulgem, T., Rushton, P.J., Robatzek, S., and Somssich, I.E.** (2000). The WRKY superfamily of plant transcription factors. *Trends Plant Sci.* **5**: 199–206.
- Eulgem, T. and Somssich, I.E.** (2007). Networks of WRKY transcription factors in defense signaling. *Curr. Opin. Plant Biol.* **10**: 366–371.
- Fields, S. and Song, O.** (1989). A novel genetic system to detect protein-protein interactions. *Nature* **340**: 245–246.
- Fuchs, J., Demidov, D., Houben, A., and Schubert, I.** (2006). Chromosomal histone modification patterns – from conservation to diversity. *Trends Plant Sci.* **11**: 199–208.
- Galletta, B.J. and Rusan, N.M.** (2015). A Yeast Two-Hybrid approach for probing protein-protein interactions at the centrosome. *Methods Cell Biol.* **129**: 251–277.
- Gao, M., Parkin, I.A.P., Lydiate, D.J., and Hannoufa, A.** (2004). An auxin-responsive SCARECROW-like transcriptional activator interacts with histone deacetylase. *Plant Mol. Biol.* **55**: 417–431.

- Gao, M., Scha, U.A., Parkin, I.A.P., Hegedus, D.D., Lydiate, D.J., and Hannoufa, A.** (2003). A novel protein from *Brassica napus* has a putative KID domain and responds to low temperature. *Plant J.* **33**: 1073–1086.
- Garcia-Ramirez, M., Rocchini, C., and Ausio, J.** (1995). Modulation of chromatin folding by histone acetylation. *J. Biol. Chem.* **270**: 17923–1792.
- Gerlitz, G., Darhin, E., Giorgio, G., Franco, B., and Reiner, O.** (2005). Novel Functional Features of the Lis-H Domain: Role in Protein Dimerization, Half-life and Cellular Localization. *Cell Cycle* **4**: 1632–1640.
- Goll, M.G. and Bestor, T.H.** (2002). Histone modification and replacement in chromatin activation. *Genes Dev.* **16**: 1739–1742.
- Gonzalez, D., Bowen, A.J., Carroll, T.S., and Conlan, R.S.** (2007). The transcription corepressor LEUNIG interacts with the histone deacetylase HDA19 and mediator components MED14 (SWP) and CDK8 (HEN3) to repress transcription. *Mol. Cell. Biol.* **27**: 5306–15.
- Grüne, T., Brzeski, J., Eberharter, A., Clapier, C.R., Corona, D.F.V., Becker, P.B., and Müller, C.W.** (2003). Crystal structure and functional analysis of a nucleosome recognition module of the remodeling factor ISWI. *Mol. Cell* **12**: 449–460.
- Grunstein, M.** (1997). Histone acetylation in chromatin structure and transcription. *Nature* **389**: 349–352.
- Gu, W. and Roeder, R.G.** (1997). Activation of p53 sequence-specific DNA binding by acetylation of the p53 C-terminal domain. *Cell* **90**: 595–606.
- Guenther, M.G., Barak, O., and Lazar, M.A.** (2002). The SMRT and N-CoR Corepressors Are Activating Cofactors for Histone Deacetylase 3. *Mol. Cell. Biol.* **21**: 6091–6101.
- Han, D., Ding, H., Chai, L., Liu, W., Zhang, Z., Hou, Y., and Yang, G.** (2018). Isolation and characterization of MbWRKY1, a WRKY transcription factor gene from *Malus baccata* (L.) Borkh involved in drought tolerance. *Can. J. Plant Sci.* **98**: 1023–1034.

- Hartley, J.L., Temple, G.F., and Brasch, M.A.** (2000). DNA Cloning Using In Vitro Site-Specific Recombination. *Genome Res.* **10**: 1788–1795.
- Haynes, S.R., Dollard, C., Winston, F., Beck, S., Trowsdale, J., and Dawid, I.B.** (1992). The bromodomain: a conserved sequence found in human, *Drosophila* and yeast proteins. *Nucleic Acids Res.* **20**: 2603.
- Hollender, C. and Liu, Z.** (2008). Histone deacetylase genes in *Arabidopsis* development. *J. Integr. Plant Biol.* **50**: 875–885.
- Hu, Y., Qin, F., Huang, L., Sun, Q., Li, C., Zhao, Y., and Zhou, D.X.** (2009). Rice histone deacetylase genes display specific expression patterns and developmental functions. *Biochem. Biophys. Res. Commun.* **388**: 266–271.
- Humphrey, G.W., Wang, Y., Russanova, V.R., Hirai, T., Qin, J., Nakatani, Y., and Howard, B.H.** (2001). Stable Histone Deacetylase Complexes Distinguished by the Presence of SANT Domain Proteins CoREST/kiaa0071 and Mta-L1. *J. Biol. Chem.* **276**: 6817–6824.
- Imai, S., Armstrong, C.M., Kaeberlein, M., and Guarente, L.** (2000). Transcriptional silencing and longevity protein Sir2 is an NAD-dependent histone deacetylase. *Nature* **403**: 795–800.
- Isenberg, I.** (1979). Histones. *Annu. Rev. Biochem.* **48**: 159–91.
- Kadosh, D. and Struhl, K.** (1998). Histone deacetylase activity of Rpd3 is important for transcriptional repression in vivo. *Genes Dev.* **12**: 797–805.
- Kadosh, D. and Struhl, K.** (1997). Repression by Ume6 Involves Recruitment of a Complex Containing Sin3 Corepressor and Rpd3 Histone Deacetylase to Target Promoters. *Cell* **89**: 365–371.
- Karimi, M., Depicker, A., and Hilson, P.** (2007). Recombinational Cloning with Plant Gateway Vectors. *Plant Physiol.* **145**: 1144–1154.

- Katiyar, A., Smita, S., Lenka, S.K., Rajwanshi, R., Chinnusamy, V., and Bansal, K.C.** (2012). Genome-wide classification and expression analysis of MYB transcription factor families in rice and Arabidopsis. *BMC Genomics* **13**: 1–19.
- Kellogg, E.A.** (2015). *Brachypodium distachyon* as a Genetic Model System. *Annu. Rev. Genet.* **49**: 1–20.
- Kim, K.-C., Lai, Z., Fan, B., and Chen, Z.** (2008). Arabidopsis WRKY38 and WRKY62 transcription factors interact with histone deacetylase 19 in basal defense. *Plant Cell* **20**: 2357–2371.
- Kornberg, R.D.** (1974). Chromatin Structure : A Repeating Unit of Histones and DNA. *Science* **184**: 868–871.
- Landy, A.** (1989). Dynamic, structural, and regulatory aspects of lambda site-specific recombination. *Annu. Rev. Biochem.* **58**: 913–949.
- Lesk, A.M.** (2014). *Introduction to Bioinformatics Fourth.* (Oxford University Press: Oxford, United Kingdom).
- Li, J., Besseau, S., Törönen, P., Sipari, N., Kollist, H., Holm, L., and Palva, E.T.** (2013). Defense-related transcription factors WRKY70 and WRKY54 modulate osmotic stress tolerance by regulating stomatal aperture in Arabidopsis. *New Phytol.* **200**: 457–472.
- Li, J., Brader, G., and Palva, E.T.** (2004). The WRKY70 Transcription Factor: A Node of Convergence for Jasmonate-Mediated and Salicylate-Mediated Signals in Plant Defense. *Plant Cell* **16**: 319–331.
- Littau, V.C., Burdick, C.J., Allfrey, V.G., and Mirsky, S.A.** (1965). The role of histones in the maintenance of chromatin structure. *Proc. Natl. Acad. Sci.* **54**: 1204–12.
- Liu, X., Yang, S., Zhao, M., Luo, M., Yu, C.W., Chen, C.Y., Tai, R., and Wu, K.** (2014). Transcriptional repression by histone deacetylases in plants. *Mol. Plant* **7**: 764–772.
- Loidl, P.** (2004). A plant dialect of the histone language. *Trends Plant Sci.* **9**: 84–90.

- Lu, Q., Tang, X., Tian, G., Wang, F., Liu, K., Nguyen, V., Kohalmi, S.E., Keller, W.A., Tsang, E.W.T., Harada, J.J., Rothstein, S.J., and Cui, Y.** (2010). Arabidopsis homolog of the yeast TREX-2 mRNA export complex: components and anchoring nucleoporin. *Plant J.* **61**: 259–270.
- Luger, K., Rechsteiner, T.J., Flaus, A.J., Waye, M.M.Y., and Richmond, T.J.** (1997). Characterization of nucleosome core particles containing histone proteins made in bacteria. *J. Mol. Biol.* **272**: 301–311.
- Lusser, A., Brosch, G., Loidl, A., Haas, H., and Loidl, P.** (1997). Identification of maize histone deacetylase HD2 as an acidic nucleolar phosphoprotein. *Science* **277**: 88–91.
- Martin, M., Potente, M., Janssens, V., Vertommen, D., Twizere, J., Rider, M.H., Goris, J., Dimmeler, S., Kettmann, R., and Dequiedt, F.** (2008). Protein phosphatase 2A controls the activity of histone deacetylase 7 during T cell apoptosis and angiogenesis. *Proc. Natl. Acad. Sci.* **105**: 4727–4732.
- Mascheretti, I., Battaglia, R., Mainieri, D., Altana, A., Lauria, M., and Rossi, V.** (2013). The WD40-Repeat Proteins NFC101 and NFC102 Regulate Different Aspects of Maize Development through Chromatin Modification. *Plant Cell* **25**: 404–420.
- Mayer, K.S., Chen, X., Sanders, D., Chen, J., Jiang, J., Nguyen, P., Scalf, M., Smith, L.M., and Zhong, X.** (2019). HDA9-PWR-HOS15 is a core histone deacetylase complex regulating transcription and development. *Plant Physiol.* **180**: 342–355.
- Mott, R., Schultz, J., Bork, P., and Ponting, C.P.** (2003). Predicting protein cellular localization using a domain projection method. *Genome Res.* **13**: 1168–1174.
- Ogata, K., Kanei-Ishii, C., Sasaki, M., Hatanaka, H., Nagadoi, A., Enari, M., Nakamura, H., Nishimura, Y., and Sarai, A.** (1996). The cavity in the hydrophobic core of Myb DNA-binding domain is reserved for DNA recognition and trans-activation. *Nat. Struct. Biol.* **3**: 178–187.
- Olins, D.E. and Olins, A.L.** (1978). Nucleosomes: The structural quantum in chromosomes. *Am. Sci.* **66**: 704–711.

- Opanowicz, M., Vain, P., Draper, J., Parker, D., and Doonan, J.H.** (2008). Brachypodium distachyon: making hay with a wild grass. *Trends Plant Sci.* **13**: 172–177.
- Pandey, R., Muller, A., Napoli, C.A., Selinger, D.A., Pikaard, C.S., Richards, E.J., Bender, J., Mount, D.W., and Jorgensen, R.A.** (2002). Analysis of histone acetyltransferase and histone deacetylase families of *Arabidopsis thaliana* suggests functional diversification of chromatin modification among multicellular eukaryotes. *Nucleic Acids Res.* **30**: 5036–5055.
- Park, H.Ji., Baek, D., Cha, J.-Y., Liao, X., Kang, S.-H., McClung, C.R., Lee, S.Y., Yun, D.-J., and Kim, W.-Y.** (2019). HOS15 Interacts with the Histone Deacetylase HDA9 and the Evening Complex to Epigenetically Regulate the Floral Activator GIGANTEA. *Plant Cell* **31**: 37–51.
- Park, J., Jin, C., Shen, M., Jin, H., Cha, J., Iniesto, E., and Rubio, V.** (2018a). Epigenetic switch from repressive to permissive chromatin in response to cold stress. *Proc. Natl. Acad. Sci.* **115**: 5400–5409.
- Park, J., Lim, C.J., Khan, I.U., Jan, M., Khan, H.A., Park, H.J., Guo, Y., and Yun, D.J.** (2018b). Identification and Molecular Characterization of HOS15-interacting Proteins in *Arabidopsis thaliana*. *J. Plant Biol.* **61**: 336–345.
- Qiu, Y. and Yu, D.** (2009). Over-expression of the stress-induced OsWRKY45 enhances disease resistance and drought tolerance in *Arabidopsis*. *Environ. Exp. Bot.* **65**: 35–47.
- Rea, S., Eisenhaber, F., O’Carroll, D., Strahl, B., Zu-Wen, S., Schmid, M., Opravil, S., Mechtler, K., Ponting, C.P., Allis, C.D., and Jenuwein, T.** (2000). Regulation of chromatin structure by site-specific histone H3 methyltransferases. *Nature* **406**: 593–599.
- Rhee, S.Y. et al.** (2003). The *Arabidopsis* Information Resource (TAIR): a model organism database providing a centralized, curated gateway to *Arabidopsis* biology, research materials and community. *Nucleic Acids Res.* **31**: 224–228.
- De Ruijter, A.J.M., Van Gennip, A.H., Caron, H., Kemp, K., and Van Kuilenburg, A.B.P.** (2003). Histone deacetylases (HDAs): characterization of the classical HDAC family.

Biochem. J. **370**: 737–749.

Rushton, P.J., Somssich, I.E., Ringler, P., and Shen, Q.J. (2010). WRKY transcription factors. *Trends Plant Sci.* **15**: 247–258.

Rushton, P.J., Torres, J.T., Parniske, M., Wernert, P., Hahlbrock, K., and Somssich, I.E. (1996). Interaction of elicitor-induced DNA-binding proteins with elicitor response elements in the promoters of parsley PR1 genes. *EMBO J.* **15**: 5690–5700.

Smith, T.F., Gaitatzes, C., Saxena, K., and Neer, E.J. (1999). The WD repeat: a common architecture for diverse functions. *Trends Biochem. Sci.* **24**: 181–185.

Song, J., Henry, H.A.L., and Tian, L. (2019). Brachypodium histone deacetylase BdHD1 positively regulates ABA and drought stress responses. *Plant Sci.* **283**: 355–365.

Sridhar, V. V., Kapoor, A., Zhang, K., Zhu, J., Zhou, T., Hasegawa, P.M., Bressan, R.A., and Zhu, J.K. (2007). Control of DNA methylation and heterochromatic silencing by histone H2B deubiquitination. *Nature* **447**: 735–738.

Tan, S., Gao, L., Li, T., and Chen, L. (2019). Genomics Phylogenetic and expression analysis of histone acetyltransferases in *Brachypodium distachyon*. *Genomics* **7543**: 1–11.

Tian, G., Lu, Q., Zhang, L., Kohalmi, S.E., and Cui, Y. (2011). Detection of Protein Interactions in Plant using a Gateway Compatible Bimolecular Fluorescence Complementation (BiFC) System. *J. Vis. Exp.*: 17–19.

Tian, L., Fong, M.P., Wang, J.J., Wei, N.E., Jiang, H., Doerge, R.W., and Chen, Z.J. (2005). Reversible histone acetylation and deacetylation mediate genome-wide, promoter-dependent and locus-specific changes in gene expression during plant development. *Genetics* **169**: 337–345.

Tripathi, P., Rabara, R.C., Langum, T.J., Boken, A.K., Rushton, D.L., Boomsma, D.D., Rinerson, C.I., Rabara, J., Reese, R.N., Chen, X., Rohila, J.S., and Rushton, P.J. (2012). The WRKY transcription factor family in *Brachypodium distachyon*. *BMC Genomics* **13**: 1–20.

- Turner, B.M.** (2000). Histone acetylation and an epigenetic code. *BioEssays* **22**: 836–845.
- Vidal, M. and Gaber, R.F.** (1991). RPD3 encodes a second factor required to achieve maximum positive and negative transcriptional states in *Saccharomyces cerevisiae*. *Mol. Cell. Biol.* **11**: 6317–6327.
- Vogel, J.P., Garvin, D.F., Mockler, T.C., Schmutz, J., Rokhsar, D., and Bevan, M.W.** (2010). Genome sequencing and analysis of the model grass *Brachypodium distachyon*. *Nature* **463**: 763–768.
- Wang, Z., Zang, C., Rosenfeld, J.A., Schones, D.E., Barski, A., Cuddapah, S., Cui, K., Roh, T.Y., Peng, W., Zhang, M.Q., and Zhao, K.** (2008). Combinatorial patterns of histone acetylations and methylations in the human genome. *Nat. Genet.* **40**: 897–903.
- Wera, S. and Hemmingst, B.A.** (1995). Serine/threonine protein phosphatases. *Biochem. J.* **311**: 17–29.
- Wilkins, O., Nahal, H., Foong, J., Provart, N.J., and Campbell, M.M.** (2008). Expansion and Diversification of the *Populus* R2R3-MYB Family of Transcription Factors. *Plant Physiol.* **149**: 981–993.
- Wu, K., Malik, K., Tian, L., Brown, D., and Miki, B.** (2000). Functional analysis of a RPD3 histone deacetylase homologue in *Arabidopsis thaliana*. *Plant Mol. Biol.* **44**: 167–176.
- Wu, K., Tian, L., Zhou, C., Brown, D., and Miki, B.** (2003). Repression of gene expression by *Arabidopsis* HD2 histone deacetylases. *Plant J.* **34**: 241–247.
- Wu, K., Zhang, L., Zhou, C., Yu, C.W., and Chaikam, V.** (2008). HDA6 is required for jasmonate response, senescence and flowering in *Arabidopsis*. *J. Exp. Bot.* **59**: 225–234.
- Yamasaki, K. et al.** (2005). Solution Structure of an *Arabidopsis* WRKY DNA Binding Domain. *Plant Cell* **17**: 944–956.
- Yang, H., Liu, X., Xin, M., Du, J., Hu, Z., Peng, H., Rossi, V., Sun, Q., Ni, Z., and Yao, Y.** (2016). Genome-Wide Mapping of Targets of Maize Histone Deacetylase HDA101 Reveals

- Its Function and Regulatory Mechanism during Seed Development. *Plant Cell* **28**: 629–645.
- Yang, X.J. and Seto, E.** (2007). HATs and HDACs: From structure, function and regulation to novel strategies for therapy and prevention. *Oncogene* **26**: 5310–5318.
- Yoon, S. et al.** (2018). PP2A negatively regulates the hypertrophic response by dephosphorylating HDAC2 S394 in the heart. *Exp. Mol. Med.* **50**: 1–14.
- You, A., Tong, J.K., Grozinger, C.M., and Schreiber, S.L.** (2001). CoREST is an integral component of the CoREST- human histone deacetylase complex. *Proc. Natl. Acad. Sci.* **98**: 1454–1458.
- Yu, J., Li, Y., Ishizuka, T., Guenther, M.G., and Lazar, M.A.** (2003). A SANT motif in the SMRT corepressor interprets the histone code and promotes histone deacetylation. *EMBO J.* **22**: 3403–3410.
- Zhang, X., Ju, H.W., Chung, M.S., Huang, P., Ahn, S.J., and Kim, C.S.** (2011). The R-R-type MYB-like transcription factor, AtMYBL, is involved in promoting leaf senescence and modulates an abiotic stress response in arabidopsis. *Plant Cell Physiol.* **52**: 138–148.
- Zhang, X., Ozawa, Y., Lee, H., Wen, Y., Tan, T., Wadzinski, B.E., and Seto, E.** (2005). Histone deacetylase 3 (HDAC3) activity is regulated by interaction with protein serine/threonine phosphatase 4. *Genes Dev.* **19**: 827–839.
- Zhang, Y. and Wang, L.** (2005). The WRKY transcription factor superfamily : its origin in eukaryotes and expansion in plants. *BMC Evol. Biol.* **5**: 1–12.
- Zhao, J., Li, M., Gu, D., Liu, X., Zhang, J., Wu, K., Zhang, X., Teixeira Da Silva, J.A., and Duan, J.** (2016). Involvement of rice histone deacetylase HDA705 in seed germination and in response to ABA and abiotic stresses. *Biochem. Biophys. Res. Commun.* **470**: 439–444.
- Zheng, Y., Ding, Y., Sun, X., Xie, S., Wang, D., Liu, X., Su, L., Wei, W., Pan, L., and Zhou, D.X.** (2016). Histone deacetylase HDA9 negatively regulates salt and drought stress responsiveness in Arabidopsis. *J. Exp. Bot.* **67**: 1703–1713.

Zhu, J., Jeong, J.C., Zhu, Y., Sokolchik, I., Miyazaki, S., Zhu, J.-K., Hasegawa, P.M., Bohnert, H.J., Shi, H., Yun, D.-J., and Bressan, R.A. (2008). Involvement of Arabidopsis HOS15 in histone deacetylation and cold tolerance. Proc. Natl. Acad. Sci. **105: 4945–4950.**

Appendices

Appendix 1: BdMYB22 Sequence

5'...ATGCTAGTGCCATATCTGTCTATCTACTACTATAAGAGATTGAAAGGAGCTGC
ACCTCCAAGGGGTTTCATCTTCGATCGATCATACTCATTTATAGAAACTACGAGGT
GGCCAACAATGTCACGGCCGAGGAAAGCAGCCATGGAAGAAGAGGATTCATCCA
CCGAGCTCCGGAGAGGCCCTGGACGCTCGAGGAAGACAACCTCCTCATGAGC
TACATTGCCTGCCACGGCGAGGGCCGCTGGAACCTCCTCGCCCGCTGCTCCGG
GTTGAAGAGGACGGGGAAGAGCTGCAGGCTGCGGTGGCTCAACTACCTGAAGC
CGGACATCAAGAGAGGCAACCTGACTGCCGAGGAGCAGCTGCTCATCCTGGAG
CTGCACGCCAAGTGGGGCAACAGGTGGTCAAGGATCGCGCAGCACTTGCCGGG
CAGGACAGACAACGAGATCAAGAATTACTGGCGGACCAGGGTGCAGAAGCAGG
CCAGGCAGCTCAACGTGGACGCAAATTCCTCCCGTGTTCCTGACGCCGTCCGCT
GCTACTGGATGCCCCGCCTGCTTGACTCGCAGTACATGGCGGCTTTCCAGGCTC
AGGCTCAGGCGGCGCATAACGCCGGAGTCGGGGACGACGATGCAGATGCAGCAG
CAAGAGCAGCAGTACAACCTGCTGCTACCCTGTTGAGAATCATAGCCCGAGCACG
GCCACGGCGTTCGACGTCCGGCGGGCGGTGGCGGAGAGATGGCGACGGCGGCGA
TGCAGCAGCAGCAACAGGCGGCGGTATTGCCGGTGCCCTGCTTCTCCGAGCTCA
ACTGGGACCTCGACGACTACCCGGCGGGCGGCGATGCTGGGAAGCAGCTGTCTT
GGGCTCGATGGGCTGGACCTTGGCCCGGCCAGGCCACGAGGCCGACTCGAC
GGCGACGCTGCTGGACTACGTCAACCACTCGAGCTTCACTTACAACCACATGAA
CTATTACTACTGCGGCGGGCGCCATGGACGACGACGGCGGGCGATCATCTTCTTCA
TGGCTCGACGACGTCCGGCGGGAGGAAGCTAGGCGAGTGGGGATCAGGAGGAA
TCTAG...3'

Appendix 2: BdWRKY24 Sequence

5'...ATGGATAACCTCCACGGAGAGGACGAAGCGCACACGCTCCCTCGCTTCTCGG
ACTTCTCATTGCCGTCCACGCCACCGCCTGCATCGCCCTTGGCCTTGCCTGACGA
TCAGCAATGCCCCCTCGCAGAGCTTCAGCAGCCGCAACCGCCGCGGTGGTGTAA
TCCTCCTCTGAACTGTCAGATGATGATGCTGCCGGAGATGGTGGACTGGTCGTCC
CTTTCCAGACGCCCGGTCTGCTGCGCCATCGGAGCGGCAGGAGGAAGCCGTG
CAGGCGGATCAGAACGGGGAGAACGACGGCGAGGCGAGCAGCGGGGGTAGTGG
CAAGGAGAAGGCTATGGGCGGCGCTGGGAGGTCGGGGAAGAAGAAGAAGA
AGGTGAGCAAGCCGCGCTTCGCATTCCAGACCAGGAGCGAGAACGATATCTTGG
ACGACGGCTACCGGTGGAGAAAGTACGGGCAGAAGGCCGTCAAGAACAGCTCCA
ACCCGAGGAGCTACTACCGTTGCACCCATCCAACGTGCAACATGAAGAAGCAGGT
GCAACGCCTGGCCAAGGATACCGACATCGTGGTGACCACATACGAGGGCACGCA
CAACCACCCATGCGATAAGCTCATGGAGGCGCTCGGCCCCATCCTGAAGCAGCTT
CAGTTTCTCTCCCGGTTCTAA...3'

Appendix 3: BdWRKY41 Sequence

5'...ATGCAGGCGCAGTCCCGTCTCATGAGCTCGGCGGCGTTCGGCGGCGGACGAG
CGGTACTACGAGGCGGTGGTGAGGGAGCTGCGGCGCGGGCACGAGCTGACGGC
GCAGCTGCAGGCGGAGGCGGCGCGCGCTGCGCGGGCAGGGCCAGGCCGAG
GCCACCGCCGCATTCATCCTGCGGGAGGTCTCCCGCGCCTTCACCGTCTGCATCT
CCATCATGGGCGGCGCCGCCCGGCCACGCCGCTCGCCGAGGCAGCGACAGCC
CCGGCGGGCGCCGCGCGCCGTCCTAGAGATGACGGCGCCCCGAGAAAAACAAT
AGAGACAAGCTCGCCCAACTCCGACGGGTACATGTGGAGGAAGTACGGCCAGAA
GAGGATCATGAAGACCAGGTTCCCAAGGTGCTACTACAGATGCAGCCACCACCGC
GAGCGCGGGTGCCCGGCCACGAAGCAGGTCCAGGAGCAGCAGCACGGCGACGG
CGCCGACCACCCGAAGACGTACCTCGTCATCTACGTCCACGAGCACACGTGCCG
CACGACGCCGCCCGCTCCGCCGAGCCCGAGGCGCCGGTTCGTGGCGCGCGGC
CGTTTAGCCCGCGACGACGACGCGGTGCCGCTGGATGGTGGCCGCGGGCGCCAA
GGAGGAGCTCGAGCGCCAGGTGCTCGTCTCGTCCCTCGCCTGCGTGCTCCAGGG
CCGCCACACCGACACTACTACTTGGGGCGGCGCGCCCGCGCCGGGGGCCGGGT
CCTCTTCGTTCGTTCGAGCTGGGCCGCGTTAGTGCTGACGACGCCGGCGCGTCTG
CTTCGCTCAACGCACTGCTGGCCACCGCGATGCCGCCGCTAACGTCGTCGCTCG
GCGCCGGGGAGGAGGAGGAGGAGCTGGACGTCATGGACTACGACGTGCCGGCC
GACACGGCGCTGTGTTTCGGCGGCCCGTTCGTACGGGATGCGTGACGACGACATG
CTGCTTTAA...3'

Appendix 4: BdHOS15 Sequence

5'...ATGGGAGGGATTACATCGGCGGAGCTCAACTTCCTCGTCTTTTCGCTACCTCC
AGGAATCCGGTTTTGTTTCATGCTGCATTTACTTTAGGGTATGAAGCAGGGATCCAC
AAGGGTGGGATAGATGGAAATGTTGTCCCCCTGGTGCTTTATCACAATTGTGC
AGAAAGGCCTCCAGTACATAGAATTGGAAGCAAATACAGATGAAAATGATGAAGA
AGTTGAGAAAGATTTTGTCTTCTGGAGCCTCTTGAAATAATCACAAAAGATGTTG
AAGAGTTGCAACAGATTGTGAAGAAGCGAAAAAGGGAGAGGCTTCAAATTGACCT
TGAAAAGGACAAGGGAAAAGAGACAGAATGCATTGAGGAGCATGAACAGCATCCT
GGAGGTGAACGTGAGAGAGAGCACCACGACAAAGAGAAAGAGCAAGAGAGGGAA
AAAGACAAAACCTGAGAGAGACAAGGCGCAAGAGAAAGAGAAAGAGAGGGAAAAA
CAACATACAGAGCGTACTGATAAGCTTAAGCATGAAGAGGATTCCCTTGCCAGTG
GAGGTCCTACACCAATGGACGTAAGTACAGGCCATGAAATTTTTAGTACGGATGT
AACCGTTTTGGAAGGGCATAGTTCAGAGGTTTTTGCCTGTGCATGGAGCCCAGCT
GGTTCTTCTAGCTTCAGGGTCAGGAGACTCAACAGCTAGAATTTGGACAATTCC
TGATGGTCCATGCGGTTCCATCCAATCATCTCCTACAAGTGTTTCATGTTCTAAAC
ATTTAAGGGCAGGACTAATGAGAAGAGCAAGGATGTCACCACACTTGACTGGAA
TGGGGAAGGAACACTATTAGCTACAGGCTCCTATGATGGGCAGGCAAGAATATGG
AGTAGGGATGGAGAGTTGAAGCAAACCTTTGTTCAAACACAAGGGACCTATATTTTC
CTTGAAATGGAATAAGAAAGGGGATTTTCTCCTAAGTGGCAGCGTAGACAAAAC
GCTATTGTGTGGGATACAAAGACATGGGAGTGCAAGCAGCAATTTGAATTTCAATC
AGCTCCAACACTAGATGTTGATTGGCGAAACAATACCTCTTTTGCAACATGCTCAA
CTGATAACATGATCTATGTTTGCAAGATTGGGGATGCACGTCCAGTTAAATCAATC
AGTGGCCATCAGAGTGAAGTTAATGCTATCAAGTGGGATCCAACCTGGTTGTTTGT
GGCTTCTTGTCTGATGATTGGACTGCAAAGATATGGAGTTTGAAGCAGGATAAAT
GTGTATACGATTTTAAAGAGCATAACCAAGGAAATATACACTATTAGGTGGAGCCCA
ACAGGTCCAGGAACAAATAATCCCAATCAACAGCTTCTTTTGGCGAGCGCATCTTT
TGATTCTTCTATCAAGCTGTGGGAAGTTGAGCATGGACGCCTTCTTTACAGCTTGG
CTGGTCATAGGCAGCCAGTTTATTCTGTGGCATTAGCCCCGATGGCGAGTACTT
GGCTAGCGGGTCCCTGGACCAAAGCCTCCATATATGGTCTGTCAAAGAAGGCAG
GATCTTGAAGACCTACAGAGGGAGCGGTGGCATTTTTGAAGTCTGCTGGAACAAA
GAAGGCAGCAAGATAGCAGCATGCTTCTCCAACAACACGGTCTGTGTCATGGATT
TCAGGATGTAG...3'

Appendix 5: BdPP2C1 Sequence

5'...ATGAGCACCGAGACGACGAGCAAGCGGGATCACGAGGCGTCCCTGCGGGA
GCTCCTGGCCGGCGGAGACAAGGAGCTGATGACCGTGGCACGCTCGGCGCGGC
GGCGCCGCCTGGA ACTCCGGCGTCTGGGGCGTACGGCGTTCGGCGGCGGCGGA
GGACGAGGGCGCGAAGAGGGTTCGCCCCGCGGGGCGCTGGACAGCTGCTCG
TCGGACTCGTCTGACTCGGCGAAGGTGACGCCGGAGCCTCAGCCGGTGTGCGT
GTCGCACGGCGCGGTCTCGGTGATCGGGCGGCGGCGGGAGATGGAGGACGCG
GTGGCCGTGGCCGCGCCGTTCTCGGCGGTGGTTGAGGGGGACGGGAAAGAGG
AGGGGTTCTTCGCGGTGTACGACGGGCACGGCGGGTCCCGCGTGGCGGAGGC
GTGCAGGGAGCGGATGCACGTGGTGCTCGCGGAGGAGGTGCAGCGGCTTCGTG
GCATCCAGCAGCAGCGGGGGAGCGGGAGCGGCCGCGACGAGGAGGAGGACGT
CATCGCAGGGTGGAAAGGAGGCCATGGCGGCCTGCTTCGCCCGGGTGGACGGCG
AGGTTCGGCGTTCGAGGACGAGGCCGAGACCGGCGAGCAGACGGTTCGGCTCCAC
GGCCGTTCGTGGCCGTTCGTGGGGCCCCGCCGCATCGTTCGTTCGCCAACTGCGGCG
ACTCCCGCGCCGTGCTCTCCCGCGCCGGCGTCCCGTGCCGCTCTCCGACGAC
CACAAGCCAGACAGACCTGATGAGATGGAAAGAGTGGAAGCAGCTGGTGGCAGA
GTTATCAACTGGAATGGATACCGTATTCTAGGAGTGCTTGCGACTTCTAGGTCAAT
AGGAGACTATTACCTGAAACCATATGTGATAGCGGAACCAGAGGTGACCGTCATG
GACCGGACAGACAAAGACGAGTTCCTCATATTAGCAAGCGACGGCTTGTGGGAC
GTTGTGTCCAACGAAGTGGCCTGCAAGATCGCAAGGAATTGCCTAAGCGGGCGG
GCGGCTTCCAAGTACCCCGAGTCCGTCTCCGGGAGCACAGCGGCCGATGCCGC
GGCGTTGCTGGTGGAGCTCGCCATGTCGCGCGGCAGCAAGGACAACATCAGCG
TTGTCGTTCGTTGAGCTGCGGCGACTGAGGAGTAGGACAGCGGCGGTGATCAAAG
AGAACCGCAGGTAG...3'

Curriculum Vitae

Name: Alberto Torrez

Post-secondary Education and Degrees: The University of Western Ontario
London, Ontario, Canada
2010-2015 B.Sc.

The University of Western Ontario
London, Ontario, Canada
2016-2019 M.Sc.

Honours and Awards: The Western Scholarship of Distinction
2010

Dean's List, Faculty of Science,
The University of Western Ontario
2015

Western Graduate Research Scholarship
2016-2018

Related Work Experience Teaching Assistant
The University of Western Ontario
2016-2019

Presentations:

Torrez, A., Song, J., Henry, H., & Tian, L. (2018) Identifying *Brachypodium distachyon* proteins interacting with histone deacetylase BdHD1. Canadian Society of Plant Biologists Eastern Regional Meeting. London, ON, Canada. [Short Communication].